frontiers | Frontiers in Materials

TYPE Review
PUBLISHED 25 April 2024
DOI 10.3389/fmats.2024.1373040

OPEN ACCESS

EDITED BY
Sumanta Kumar Karan,
The Pennsylvania State University (PSU), United States

REVIEWED BY
Nur Amin Hoque,
Indian Institute of Science Education and Research Mohali, India
Ritamay Bhunia,
Hanyang University, Republic of Korea

*CORRESPONDENCE
Zhiqiang Song,
zqsong@cwxu.edu.cn

RECEIVED 19 January 2024
ACCEPTED 09 April 2024
PUBLISHED 25 April 2024

CITATION
Song Z, Hou R and Jiang F (2024), Recent progress in piezoelectric thin films as self-powered devices: material and application.
Front. Mater. 11:1373040.
doi: 10.3389/fmats.2024.1373040

Recent progress in piezoelectric thin films as self-powered devices: material and application

Zhiqiang Song[1]*, Rongxi Hou[1] and Feng Jiang[1,2]

[1]School of Automation, Wuxi University, Wuxi, Jiangsu, China, [2]School of Electrical and Information Engineering, Changzhou Institute of Technology, Changzhou, Jiangsu, China

Piezoelectric materials have become a key component in sensors and actuators in many industrial fields, such as energy harvesting devices, self-powered structures, biomedical devices, nondestructive testing, owing to the novel properties including high piezoelectric coefficient and electromechanical coupling factors. Piezoelectric thin films integrated on silicon substrates are widely investigated for their high performance and low manufacturing costs to meet the requirement of sensor networks in internet of things (IoT). The aim of this work is to clarify the application and design structure of various piezoelectric thin films types, synthesis methods, and device processes. Based on latest literature, the process of fabricating thin film sensors is outlined, followed by a concise overview of techniques used in microelectromechanical systems (MEMS) processing that can integrate more complex functions to obtain relevant information in surrounding environment. Additionally, by addressing piezoelectric thin films sensors as a cutting-edge technology with the ability to produce self-powered electronic devices, this work delivers incisive conclusions on all aspects of piezoelectric sensor related features. A greater understanding of piezoelectricity is necessary regarding the future development and industry challenges.

KEYWORDS

piezoelectric, thin films, self-powered devices, wearable sensors, MEMS

1 Introduction

Thin film sensors are widely used in aerospace, mechanical manufacturing, civil engineering, mining and other industrial fields (Zhang et al., 2021a; Shalabi et al., 2022; Song et al., 2022). With thickness in range from a few hundred nanometers to tens of microns, thin film sensors can be integrated directly onto surface of component under test without changing environment inside the device, making integrated structure and sensing fabrication easy to implement (Yu et al., 2023; Yue et al., 2023). Using large area film preparation technology, thin film strain resistance is placed on metal elastic substrate, with high precision, good creep, and strong anti-interference ability, etc. (Agarwala et al., 2017; Kirthika et al., 2017; Qiao et al., 2018; Russell et al., 2022). Through the development of new material systems and new physical mechanisms, piezoelectric thin film sensors have made great progress in sensitivity, response range, response time, linearity, hysteresis, and stability, and have shifted from the development of a single sensor to the development and optimization of the system level. Piezoelectric materials play key roles in various electronic devices such as wireless sensor networks, mobile electronics, wearable and implantable biomedical devices. Piezoelectric thin films have found a broad range of lab-on-chip

applications. Generated power from piezoelectric sensor can be used to drive low powered electronic devices. By combining hardware and software technologies, piezoelectric film sensors form an intelligent sensing platform for the internet of things (IoT), which will be widely used in health monitoring, home interconnection and intelligent manufacturing, et al. (Yamamoto et al., 2016; Zhang et al., 2021b; Liu et al., 2023a).

Internet of things is considered to be the third major innovation in information technology after the emergence of computers and internet (Fan et al., 2022; Zhang et al., 2023a; Kalyanasundaram Balasubramanian et al., 2023). Through connections between different entities, data is shared and numerous devices on the network are able to interact and collaborate (Zhao et al., 2020a; Chionh et al., 2020; Liu et al., 2023b; Zhang et al., 2023b; Huang et al., 2023; Portilla et al., 2023; Tsakanikas et al., 2023). There are three main layers in architecture of IoT, including perception layer, network layer and application layer (Uslu et al., 2020). The sensing layer obtains data from the external physical world through various means such as sensors or digital cameras, and transmits it through a series of short-range transmission technologies such as radio frequency identification (RFID), industrial fieldbus, Bluetooth and infrared (Liu et al., 2020; Mrabet et al., 2020; Cui et al., 2021; Liu et al., 2022a). With the rapid development of intelligent manufacturing, intelligent transportation, smart city and wearable technology (Atlam et al., 2018; Eini et al., 2021; Lopez-Castaño et al., 2021; Mondal and Rehena, 2022; Debeuckelaere et al., 2023), the IoT has a great demand for the miniaturization, integration, and low power consumption of sensors (Botta et al., 2016; Silvano and Marcelino, 2020). At present, new flexible sensors have been used in medical devices, such as electronic skin, personal medical devices and prosthetics (Hwang et al., 2015; Liao et al., 2015; Chen et al., 2016; Choi et al., 2016; Chortos et al., 2016; Ge et al., 2016; Park et al., 2016; Zang et al., 2016). Recently, the proliferation of new piezoelectric crystals, piezoelectric polymers, and lead-free piezoelectric materials has led to significant improvements in electromechanical coupling response, material properties, and applications. As shown in Figure 1, this work will present the development status of thin film sensors from four aspects: material selection, synthesis, sensor processing technology, and sensor application.

2 Piezoelectric materials

Piezoelectric materials present a mechanical-electric coupling effect that can cause mechanical bending when electric field applied and can also cause electric charges to build up on the two ends of material when it is bent (Hinchet et al., 2018). Owing to both positive and negative piezoelectric effects, piezoelectric materials can be used as both sensors and actuators (Joseph et al., 2018; Antony Jeyaseelan and Dutta, 2020; Ni et al., 2022). In 1880, brothers Pierre and Jacques Curie demonstrated the direct piezoelectric effect for the first time. They apply mechanical stress to a variety of single crystals such as tourmaline, quartz, topaz and Rochelle salt. The stress applied to the crystal produces a measurable surface charge. However, they did not initially show that it was also possible to generate electric-induced strain. The following year, mathematician Gabriel Lippmann predicted the inverse piezoelectric effect, which the Curie brothers soon confirmed. Through MEMS process, piezoelectric thin films can be integrated on silicon substrate to make tiny sensors and controller. Recently, due to the high piezoelectricity, biocompatibility, and low dielectric constant, bio-piezoelectric materials have become one of the most potential smart materials in biology (Kim et al., 2020; Chen et al., 2023a). In this part, the classification of piezoelectric materials will be introduced in detail.

In this work, we considered the most common crystal structures in piezoelectric applications. From a commercial perspective, polycrystalline ferroelectrics are possible for large-scale production. Due to the arbitrary orientation of crystals in ceramics, symmetry breaking elements must be introduced externally in order to obtain piezoelectric response. Therefore, ferroelectric materials can be used for piezoelectric ceramics. They can be polarized, meaning that their polar axis can be aligned with an external electric field, resulting in the required reversal of symmetry being disrupted. Therefore, among the 20 non centrosymmetric crystal point groups with potential to exhibit piezoelectric properties, piezoelectric ceramic materials only need to consider 10"polar" groups: 1 (triclinic), 2, m (monoclinic), 2 mm (orthorhombic), 3, 3 m (rhombohedral), 4, 4 mm (tetragonal), 6, and 6 mm (hexagonal). Among all possible crystal structures, perovskite structure may be the most common and technically relevant. The chemical composition of perovskite is ABO_3. This structure can be described as a simple cubic cell with a large cation (a site) at the corner, a small cation (B site) at the center of the body, and oxygen at the center of the face.

2.1 Piezoelectric crystal

Piezoelectric crystals commonly found in various applications include quartz and water-soluble crystals such as sodium potassium tartrate, diammonium ethylene tartrate, dipotassium tartrate, and potassium sulphate (Zu et al., 2016; Lutjes et al., 2021; Dong et al., 2022). For polycrystalline, notable piezoelectric materials include barium titanate, zirconium lead titanate, and lead niobium magnesium oxide, et al. (Okayasu and Watanabe, 2016; Wu et al., 2016; Kumar et al., 2023; Shi et al., 2023). In 1997, large S-E strain was found in lead based relaxor ferroelectric crystals, which is widely regarded as a significant advancement in piezoelectric materials (Xu et al., 2000). Sm-doped lead niobium magnesium oxide-lead titanate crystals exhibit high piezoelectric coefficients exceeding 4,000 pC/N and dielectric constants with value of 12,000. The uniformity of crystals rod properties is enhanced by leveraging the sub-condensation properties of Sm elements during crystal growth. This advancement establishes a solid basis for the development of piezoelectric crystals suitable for high frequency medical ultrasound probes and high precision actuators (Li et al., 2019).

Barium titanate ($BaTiO_3$, BT) presents high dielectric properties, which is extensively manufactured as high-frequency circuit components (Karvounis et al., 2020; Chen et al., 2022), as shown in Figure 2A. The thermal properties of BT can be enhanced by the process of Pb and Ca co-dopant (Hasan et al., 2023). The

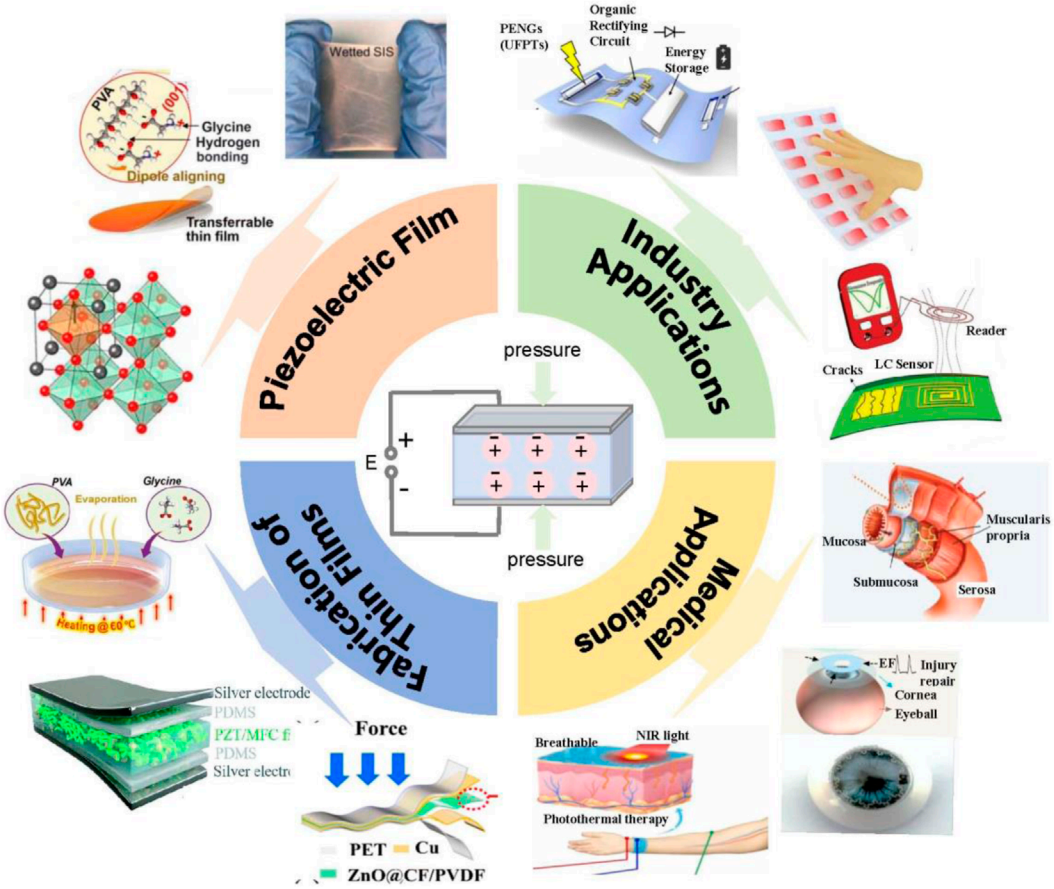

FIGURE 1
Framework of piezoelectric thin-film sensors, including materials, processing, and applications.

enhanced piezoelectric properties in BT-based ceramics can be achieved by use of ion-pair effect and A/B-site synergistic doping modification (Xie et al., 2022), as seen in Figure 2B. High d_{33} value (30.5 pC/N) and Curie temperature (Tc = 657°C) were found in Bi_4Ti_3-x $(Zn_{1/3}Nb_{2/3})xO_{12}$ ceramics. Additionally, the aligned ferroelectric domains demonstrate remarkable temperature stability (Xie et al., 2022). Lead zirconate titanate (PZT) is a solid-state solution consisting of lead titanate ($PbTiO_3$) and lead zirconate ($PbZrO_3$), which is extensively used as transducers materials owing to consistent piezoelectric properties and high Curie temperature (Tan et al., 2019), as shown in Figure 2C. The ceramics exhibit various features, after small amounts of dopant, such as niobium, antimony, tin, manganese, tungsten, et al. (Koh et al., 2022; Chen et al., 2023b; Habeeb Khan et al., 2023). With the protection of environment, lead free piezoelectric materials are widely investigated. Quartz crystals integrated on silicon substrate is shown in Figure 2D. Figure 2E illustrates the schematic structure of AlN crystals (Fei et al., 2018). Commonly used lead-free piezoelectric systems include KNN-BNT, KNN-BT, BNT-BT, BKT-BT, BNT-BT-KNN, and BNT-BKT (Mayamae et al., 2017; Zhang et al., 2022a; Wang et al., 2022; Safari et al., 2023; Tai et al., 2023). The S-E strain in (K, Na) NbO_3 polycrystalline is enhanced by solid solution near phase border, which undergoes a phase transition, as shown in Figure 2F.

2.2 Piezoelectric polymers and composites

Polar polymers like polyvinylidene fluoride (PVDF) are good examples of polymer piezoelectric materials, which show low sound resistance, and can be made into thin parts (Wang et al., 2023a). Polymers can be used directly in actuator and sensor, owing to electrical and mechanical energy conversion (Takahashi and Tadokoro, 1980; Koseki et al., 2012; Bouad et al., 2022; Zhang et al., 2023c). Due to big dipole moments, β phases PVDF exhibit high dielectric and piezoelectric properties (Nasir et al., 2006; Satapathy et al., 2011; Huang et al., 2021). The d_{33} value can reach up to 62pC/N in β-phase PVDF films (Huang et al., 2021). Polytetrafluoroethylene (PTFE) is resistant to acids, alkalis, and a wide range of organic solvents (Dhanumalayan and Joshi, 2018; Niu et al., 2022). Neutral PTFE particles (d > ~1–5 μm) can be turned into piezoelectric electrets using an easy-to-use ultrasound process at faster rate than piezoelectric catalysts (Wang et al., 2021).

Compared with the piezoelectric polymer, the inorganic piezoelectric ceramic particles have high piezoelectric constant and low breakdown strength. Therefore, through adding piezoelectric ceramics powder into polymers, the composite shows high piezoelectric coefficient and low poling field (Hema Malini et al., 2022). Compared with individual piezoelectric components, piezoelectric composite materials can overcome the temperature

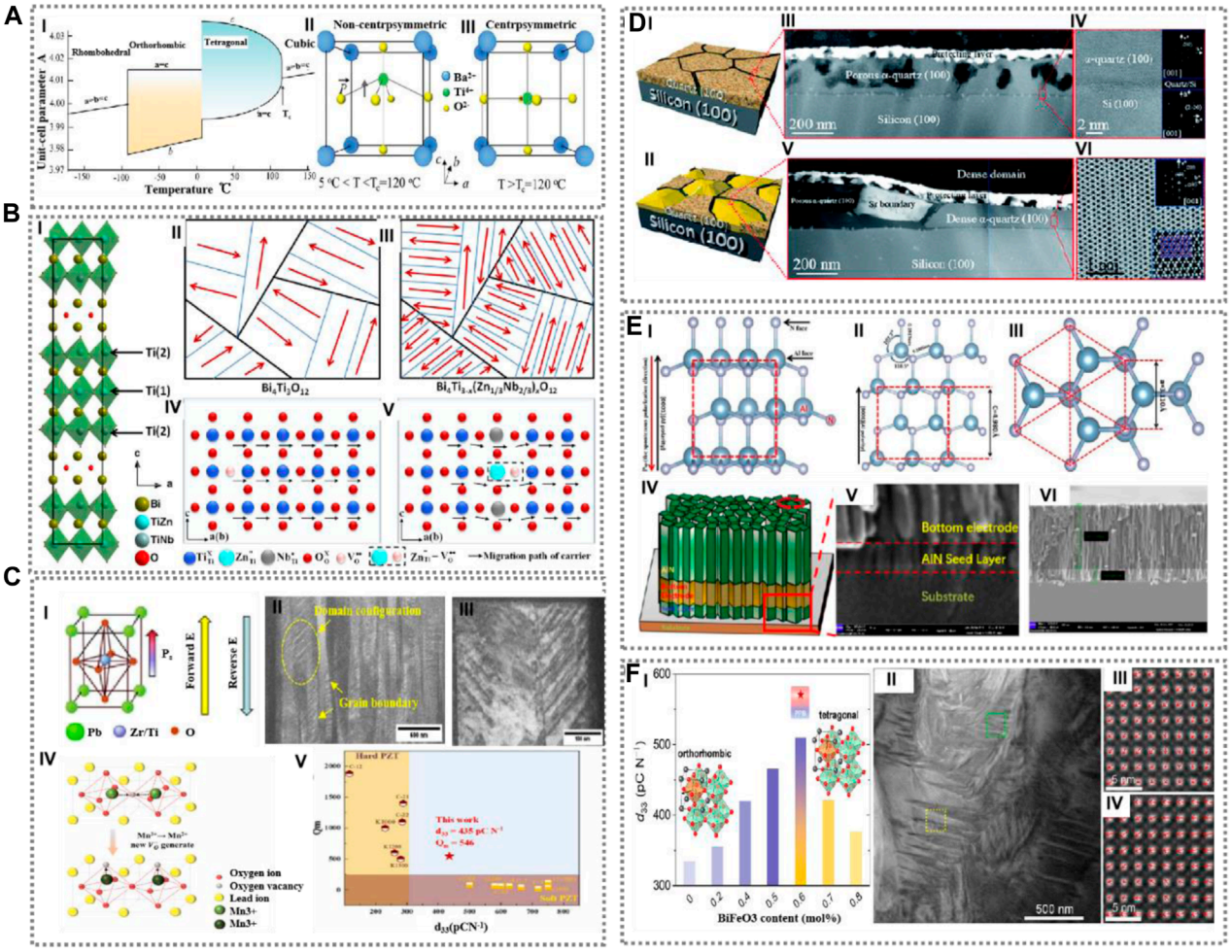

FIGURE 2
Crystalline unit cell and microstructure of piezoelectric materials. **(A)**-I: Non centrosymmetric unit cell structure of $BaTiO_3$ for tetragonal phase (below Curie temperature), and centrosymmetric unit cell structure of $BaTiO_3$ for cubic phase (above Curie temperature). **(A)**-II and III: Variation of cell volume at different temperatures in $BaTiO_3$ crystals (Karvounis et al., 2020). **(B)**-I, II, and III: Schematic of BT-based crystal structure and ferroelectric domain walls. **(B)**-IV and V: Schematic migration model of the charge carriers (Xie et al., 2022). **(C)**-I: Relationships between polarization and applied electric field in PZT. **(C)**-II and III: Microstructure of as-deposited PZT thin film (Tan et al., 2019). **(C)**-IV: Schematic diagram of Mn^{3+} valence change to generate oxygen vacancies and strengthen pinning (Chen et al., 2023b). **(C)**-V: Comparison of Mn-doped PSN-PZT among other commercially PZT-based ceramics (Hao et al., 2019). **(D)**: Two different microstructures in α-quartz (100) film on silicon substrate (Zhang et al., 2019). **(E)**-I, II, and III: Schematic illustration of wurtzite structure of AlN. **(E)**-IV: Schematic diagram of functional AlN layer deposited on AlN seed layer. **(E)**-V and VI: Cross-section image of AlN layer. **(F)**-I: Piezoelectric coefficient d_{33} of KNN-BF solid solutions. **(F)**-II, III, and IV: Scanning transmission electron microscopy (HAADF-STEM) image of KNN-BF crystals (Zhang et al., 2022a).

boundary of piezoelectric polymers and the inherent brittleness of inorganic piezoelectric biomaterials, while also allowing for large-scale manufacturing. The addition of barium titanate particles contributes the formation of β-phase in PVDF membrane (Khan et al., 2021), as shown in Figure 3A. Guan measured heel pressure in a new hybrid film made of lead zirconate titanate powder and micro fibrillated cellulose (PZT/MFC), which is a bendable film made with a polarization process (Guan et al., 2022), as presented in Figure 3B. Li made synthetic fabric films out of mixtures of PVDF and cellulose acetate (CA). Electrostatically spun PVDF/CA fiber membranes (EFMs) were used to make flexible nanogenerators (Li et al., 2022a), as shown in Figure 3C. For TiO_2/SiO_2/polymethyl methacrylate (PMMA)/PVDF composites, the β -phase content in the PVDF matrix increase from 19% to 43% as TiO_2 or SiO_2 contents increase from 0% to 5%, which made piezoelectric properties of PVDF better (Zhao et al., 2012; Li et al., 2013). A flexible ZnO/PVDF hybrid piezoelectric films with TiO_2 particles addition were used to make nanogenerator, showing a voltage is 2.3 times higher than that of pure PVDF nanogenerator (Kim et al., 2018). In a three-phase hybrid nanogenerator out of PVDF, ZnO, and BT nanorods, the output increase from 3 V to 12 V (Sabry and Hussein, 2019). The addition of nanoparticles can improve the crystallinity and the mount of β phase of the fiber films (Fakhri et al., 2019; Ye et al., 2021). Kar made a new bendable piezoelectric nanogenerator based on two-dimensional SnO_2 nanosheets and PVDF composites, and presented a high output rate with value of 16.3% (Kar et al., 2019). A three-dimensional hybrid nanostructure of MnO2/Gr/multi-walled

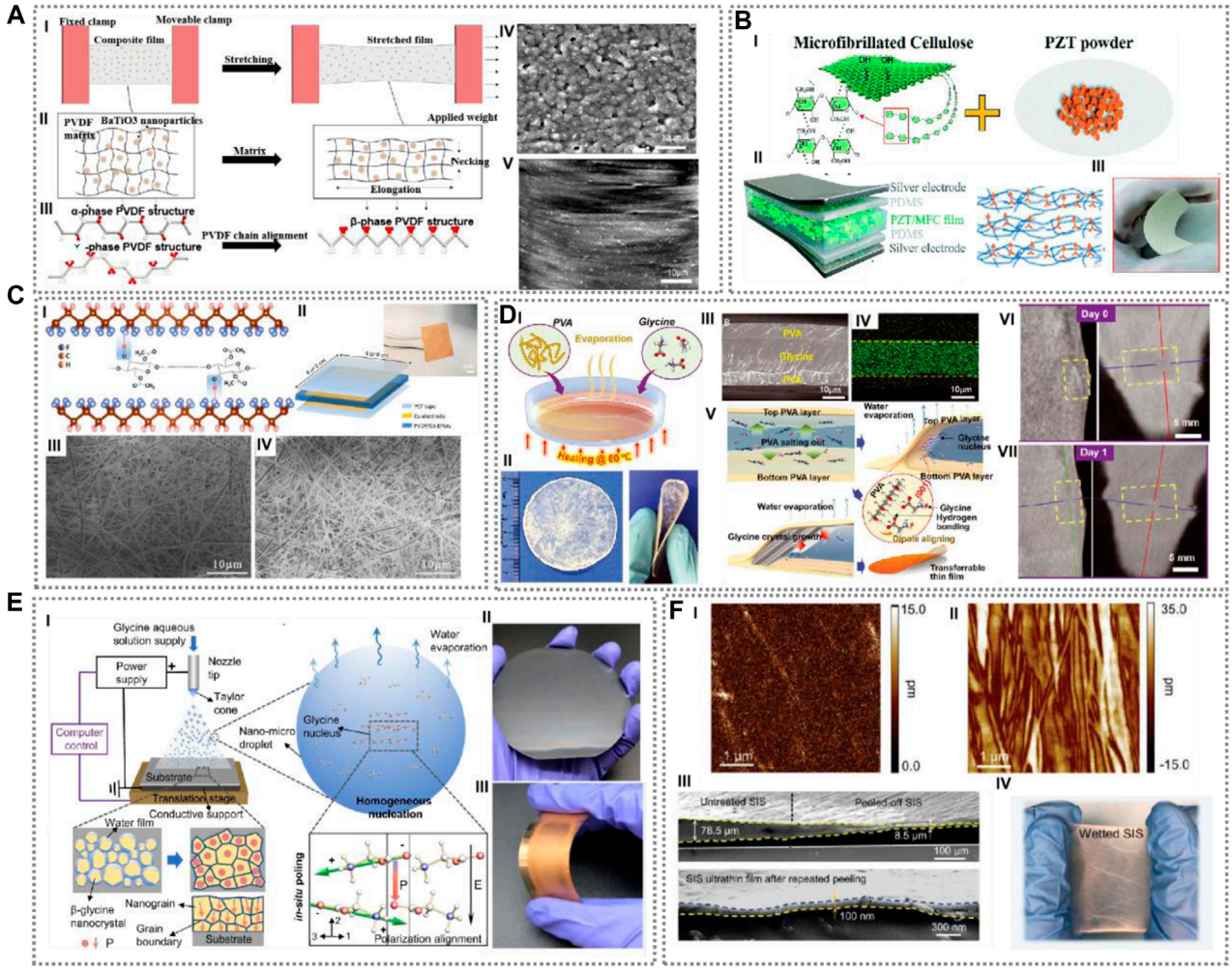

FIGURE 3
(A)-I, II, and III: Conceptual illustration of $BaTiO_3$-PVDF composite structure before and after stretching, including the applied uniaxial stretching mechanism, polymer matrix elongation, and conversion of α and γ phase PVDF to β phase. **(A)**-IV and V: SEM images of composite films before and after stretching (Khan et al., 2021). **(B)**: Structure of thin films mixed of PZT powder and MFC (Guan et al., 2022). **(C)**-I: Chemical interactions between the CA and PVDF molecular chains. **(C)**-II: Picture of PVDF/CA PENG. **(C)**-III and IV: SEM images of pure PVDF and PVDF/CA (Li et al., 2022a). **(D)**-I: Schematic synthesis approach of piezoelectric glycine-PVA films over a large area. **(D)**-II: Photographs of wafer-sized as-grown film (left) and largely curved film showing the flexibility (right). **(D)**-III and IV: Cross-sectional SEM image and EDS mapping of a sandwich-structured films. **(D)**-V, VI, and VII: Crystallization process of glycine-PVA sandwich thin films (Yang et al., 2021). **(E)**-I: Schematic of bio-organic films printer and the synthesis of β-glycine nanocrystalline films. **(E)**-II: Photographs of films on 4-inch silicon wafer. **(E)**-III: Films on flexible gold-coated polyethylene terephthalate (PET) substrate (Zhang et al., 2023d). **(F)**-I and II: PFM image of SIS films. **(F)**-III: Cross-sectional SEM image of untreated SIS and peeled-off SIS films. **(F)**-IV: Picture of SIS ultrathin films (Zhang et al., 2022b).

carbon nanotubes was also used to enhance the electrical properties of PVDF (Yang et al., 2018). Recently, nano-piezoelectric materials, including quantum dots, two-dimensional materials and topological insulators, have been added to PVDF to improve the power output of self-powered wearable devices and achieve excellent output performance (Hoque et al., 2017; Biswas et al., 2019; Bagchi et al., 2020; Shi et al., 2020; Saikh et al., 2021; Sarkar et al., 2023a; Sarkar et al., 2023b). A 2D halide chalcogenide transverse heterostructures prepared by liquid-phase epitaxy, which strongly suppressed the in-plane ionic diffusion in 2D halide chalcogenides by doping rigid π-conjugated organic ligands (Shi et al., 2020).

2.3 Bio-piezoelectric materials

Piezoelectric biomaterials are naturally suited for coupling mechanical and electrical forces in biological systems for real-time sensing, actuation, and power generation *in vivo*; however, large-scale synthesis and alignment of piezoelectric phases in bio-piezoelectric thin films still a major challenge (Swagata et al., 2017; Hoque et al., 2018; Lay et al., 2021; Sarkar et al., 2021; Das et al., 2022; Mondal et al., 2022). Piezoelectric biomaterials are low symmetry, highly ordered structures, lacking inversion centers. Therefore, linear electromechanical coupling is an inherent functional characteristic of most biomolecules. Piezoelectricity has

been demonstrated in various biomaterials, such as wood and bone, as well as fibrillar proteins such as collagen, chitin, and elastin, which exist in highly ordered crystalline molecular forms in mammalian tissues. The classical piezoelectric principle has been applied to similar uniaxial oriented bioactive polymers, such as poly (lactic acid) (PLLA), poly (lactic acid) γ- Benzylglutamic acid (PBG) and cellulose 3. These biodegradable polymers have been used as piezoelectric implants to promote pure and composite forms of bone formation. As is well known, the surface charge and wettability of the scaffold control the interaction between the material cell interfaces. The shape of the bracket can be controlled through various manufacturing processes, and the additional functionalization of the material can be used to fix biochemical substances. The morphological characteristics, piezoelectric constant, and ferroelectricity of piezoelectric materials can be modified to meet specific requirements. Nanostructured PZT in the form of nanoribbons or nanowires has been developed and applied in the construction of biomedical and energy harvesting devices. However, due to its cytotoxicity, the application of PZT ceramics in tissue engineering is limited. Therefore, lead-free piezoelectric ceramics have been developed to reduce people's concerns about lead exposure to toxic environments.

Two simple, portable, cost-effective, biocompatible, and environmentally friendly piezoelectric nanogenerators (PENGs) were designed using naturally biodegradable mud volcanic clay from the Andaman and Nicobar Islands in India. The output voltage of MPENG and BPENG is ~85V, and the short-circuit current is ~1.6 μA. The output voltage is~125 V, and the short-circuit current is ~1.9 μA. The power density is 4115 respectively $\mu W/cm^3$ and 7187 $\mu W/cm^3$ (Das et al., 2022). Recently, a generator can produce electrical signals when squeezed by body movement, which will lead to a wide range of uses for muscle-powered electromechanical treatments (Chorsi et al., 2019). A self-assemble method using lysine as a piezoelectric generator has presented a way to make a product through chemical qualities of a material, as shown in Figure 3D. This fast self-assembly technology could greatly cut the cost of these kinds of gadgets and make them much easier to get and use.

A biodegradable poly nanofiber was designed to get chondrocytes and cartilage tissue grow back, which can create piezoelectric effect when stressed or loaded in a joint (Yang et al., 2021), as shown in Figure 3E. Without extra battery, cartilage can be regrown by implanting the disposable PLA support and producing microcurrents while walking. After 1–2 months of exercise, hyaline cartilage grown back in rabbits with serious osteoarticular flaws that had received piezoelectric scaffold grafts. The fully healed cartilage tissue was surrounded by a large number of chondrocytes and type II collagen. An active self-assemble method to shape piezoelectric biomaterial films is presented in Figure 3F. Nanoconfinement caused uniform nucleation, which will get rid of dependence on interface of films (Liu et al., 2022b). During the process of van der waals exfoliation, ultrathin films are thinned to effective piezoelectric domain thickness (Zhang et al., 2023d).

3 Synthesis of piezoelectric thin films

There are many ways to make piezoelectric thin films, such as vacuum evaporation, sputtering coating, chemical vapor deposition, molecular beam epitaxy, and sol-gel method. Here, a list of the most common ways to make thin films, such as AlN, KNN, ZnO, PZT, and PVDF, et al.

3.1 AlN piezoelectric films

AlN thin films is a hot topic of research in RF field because they are often used in high frequency sound resonators. These films can be made by blasting with a magnetron. Zhao reported a high-quality bendable AIN piezoelectric film made with micro- and nano-fabrication technology (Zhang et al., 2022b). The Mo/AIN/Al structure on silicon {100} was made by blasting, and then ion etching was used to remove the silicon used as a support to get a bendable Mo/AIN/Al sandwich film (Zhao et al., 2020b). Wen used an RF magnetron sputtering method with aluminum-rich AlN (Al-AlN) targets to make AlN films on Si surfaces with a low number of defects (Wen et al., 2022). Al vacancies and O impurity defects in AlN films can be cut down with the help of modulation in AlN films. Patidar used a highly detailed oblique angle deposition method to make c-axis oriented AlN (0002) films with reactive metal ions that were timed with HiPIMS (Patidar et al., 2023). As shown in Figure 4A, combining HiPIMS with a small substrate bias of only −30 V greatly improves the crystalline quality and texture of the films. Process gas doping and point defect formation can be further reduced by synchronizing the negative substrate bias with Al. The films have a clear out-of-plane pattern and regular grain polarization.

One of the best ways to enhance piezoelectric response of AlN thin films is to mix it with other elements to make conformal films. By mixing transition metals (TMs, TM = Sc, Cr, Sr, Mo, Ru, and Rh, etc.), TM-N bonds become weak and move the TM atoms closer to the centers of the three nearby N atoms. It was found that the place of the TMs was strongly linked to their group number (Akiyama et al., 2009a; Akiyama et al., 2009b; Luo et al., 2009; Liu et al., 2013; Mayrhofer et al., 2015; Hu et al., 2018; Manna et al., 2018; Yanagitani and Jia, 2019; Fiedler et al., 2021; Feng et al., 2022; Lv et al., 2023a; Patidar et al., 2023; Zha et al., 2023). For Mo dopant, piezoelectric coefficient d_{33} of AlN: Mo (3.46%) films reached to 7.33 pm/V (Feng et al., 2022). In the past few years, research has been done to figure out how to make high-quality mixed epitaxial films of AlN. Using nanopatterned AlN/sapphire templates with regular hexagonal holes, the dislocation, etch pit density in AlN heteroepitaxial thin films was reduced to about 104 cm^{-2}, which is close to value in AlN bulk crystals, by controlling the separation and grouping of the columns (A strategy for obtaining AlN, 2023).

3.2 PZT piezoelectric films

PZT piezoelectric thin films are widely used, which can be made by various methods, such as magnetron sputtering (Beklešovas et al., 2022), chemical vapour deposition (Aratani et al., 2001), molecular beam epitaxial growth, hydrothermal synthesis (Bian et al., 2016), pulsed laser deposition (Gatabi et al., 2017), and sol-gel (Lee et al., 2021).

High performance PZT films were obtained on fluorine-doped tin oxide (FTO)-coated aluminum borosilicate glass (AG) surfaces using a modified sol-gel method (Di Marco et al., 2023). Liu made

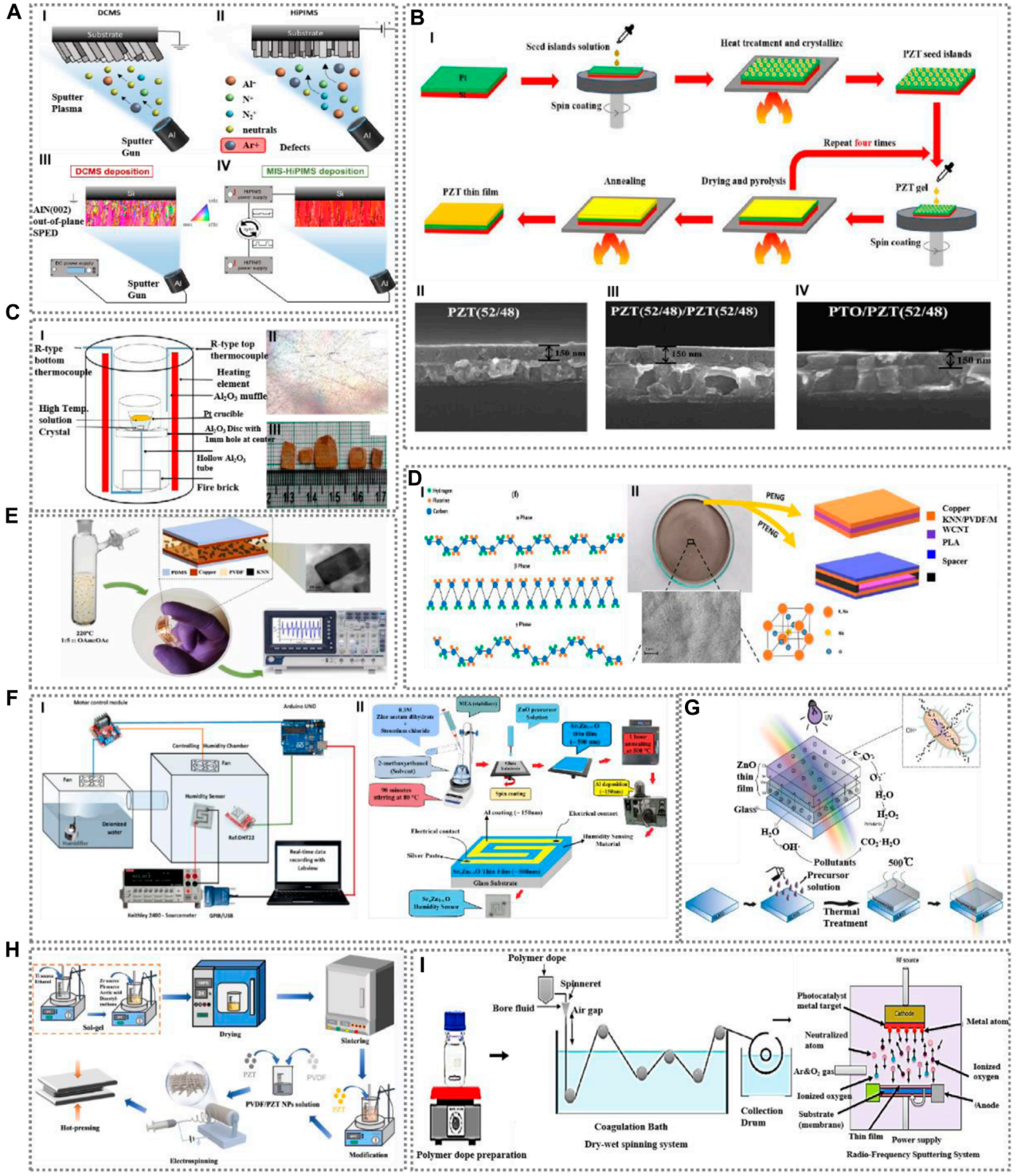

FIGURE 4
(A): Schematic of AlN films growth using DCMS and HiPIMS methods (Patidar et al., 2023). **(B)**-I: Crystal growth diagram of PZT ferroelectric thin films with seed islands. **(B)**-II, III, and IV: Cross-section images of PZT (52/48) and PTO/PZT films (Liu et al., 2022). **(C)**: BNBT crystals grown by self-flux method (M et al., 2020). **(D)**-I and II: Synthesized KNN/PVDF/MWCNT films and PENG (Abdullah et al., 2021). **(E)**: Schematic of fabrication procedure of KNN/PVDF-based nanogenerator (Nair et al., 2022). **(F)**: Schematic of synthesis and fabrication of $Sr_xZn_{1-x}O$ nanostructured humidity sensor (Algün et al., 2023). **(G)**: Schematic of transparent ZnO thin films grown on glass substrates (Cuadra et al., 2023). **(H)**: Schematic illustration of PVDF/PZT NPs fiber films preparation (Yuan et al., 2023). **(I)**: Schematic preparation of Cu_xO/PVDF films (Zakria et al., 2023).

Pb $(Zr_{0.52}Ti_{0.48})O_3$ thin films with islands of $Pb(Zr_xTi_{1-x})O_3$ solid species using the sol-gel method (Liu et al., 2022c), as shown in Figure 4B. The $Pb(Zr_{0.52}Ti_{0.48})O_3$ films have been changed by $Pb(Zr_xTi_{1-x})O_3$ crystalline seed islands with different Zr/Ti ratios, presenting higher dielectric constant, lower coercive electric field, and less leakage current density. Furthermore, $PbZr_{0.52}Ti_{0.48}O_3$ thin films were successfully made by the sol-gel method at ultra-low temperature (450 °C) in an oxygen plasma-assisted environment in Ref. (Li et al., 2023a), which can be used to make modern CMOS devices.

After fast thermal annealing at 620°C, a high energy storage density of 10.0 J/cm^3 was obtained in $PbZr_{0.52}Ti_{0.48}O_3$ (PZT)/$PbZrO_3$ (PZ) hybrid films on a $LaNiO_3/SiO_2/Si$ substrate synthesized by sol-gel method (Yang et al., 2023). Rhun grown thick PZT films on platinum-coated silicon plates using sol-gel method, and move PZT films and ITO electrodes onto glass substrates (Le Rhun et al., 2022). In visual range, the average amount of light that get through PZT stacks on glass was 70%, which makes it possible to make clear piezoelectric motors on glass for high-performance haptic devices and other new uses, like self-cleaning or making smart windows.

3.3 Relaxor ferroelectric crystals

Flexible piezoelectric films composed of lead magnesium niobate and lead titanate (PMN-PT) and multi-walled carbon nanotubes (MW-CNTs) were prepared in polyvinylidene fluoride (PVDF) matrix for green energy harvesting and self-power supply (Das et al., 2017; Das et al., 2018). Fully artificial transparent Sm-doped $Pb(Mg_{1/3}Nb_{2/3})O_3$-$PbTiO_3$ (Sm:PMN-PT) thin films on mica substrates were fabricated by one step sol-gel process. The films show high d_{33} with value of 380 pm/V, indicating potential use for mechanical energy gathering, motion tracking, and human-computer interaction (Das et al., 2017; Lv et al., 2022).Using a self-flux method, large size of lead free 0.94 $(Bi_{1/2}\ Na_{1/2})\ TiO_3$ - $0.06BaTiO_3$ (BNBT) piezoelectric crystals were grown by self-flux method, as shown in Figure 4C.

3.4 KNN piezoelectric films

Several methods are used to make KNN-based piezoelectric films, such as alkaline methods, pulsed laser methods, and sol-gel methods (Bai et al., 2011; Khorrami et al., 2017; Akmal et al., 2018; Sharma et al., 2019; Fast et al., 2020; Kovacova et al., 2020; Abdullah et al., 2021; Cheng et al., 2022; Nair et al., 2022). Because of the advances in flexible piezoelectric nanogenerators, alkali metal niobates have received a lot of attention and are considered an environmentally friendly choice for lead-based piezoelectric materials. Abu used potassium sodium niobate (KNN) to make an energetic film (Abdullah et al., 2021), as shown in Figure 4D. It was used to make copper plates for a piezoelectric nanogenerator (PENG). It was also shown that KNN-based energy films could be used for multipurpose uses (like force and pressure sensors) and lead-free energy harvesting. As shown in Figure 4E, Nair made a lead-free foldable piezoelectric nanogenerator out of KNN-PVDF nanocomposites (Nair et al., 2022). Cheng investigated the strengthening effect of CuO-doped KNN-based ceramics, and found that Cu doping strongly upset the ferroelectric ordering (Cheng et al., 2022). An idea of using solution synthesis to keep the alkali chemistry of the Mn-doped KNN films uniform was given in Ref. (Kovacova et al., 2020). A uniform grain size of 80 nm and a leakage current density of $2.8 * 10^{-8}$ A/cm^2 under an electric field of up to 600 kV/cm were obtained in chemically uniform KNN thin films.

3.5 ZnO piezoelectric films

ZnO thin films can be made by blasting with an RF magnetron (Li et al., 2018; Sonklin et al., 2022; Algün et al., 2023; Cuadra et al., 2023; Kahveci et al., 2023; Murthy et al., 2023; Toma et al., 2023). {002} oriented Li-doped ZnO thin films on SiO_2/Si was obtained using RF magnetron sputtering, when the sputtering power was 220 W and the Li-doped concentration was 5% (Li et al., 2018). As shown in Figure 4F, nanoparticles of undoped zinc oxide (ZnO) and Sr_xZn_{1-x} (x = 0.01, 0.02, 0.03, 0.04, and 0.10) were synthesized using the sol-gel method (Algün et al., 2023), as shown in Figure 4F. As shown in Figure 4G, high crystallinity ZnO thin films were synthesized by a spray pyrolysis method, show antibacterial qualities when exposed to UV light (Cuadra et al., 2023). Transparent conductive films were made by sputtering Ga-doped and (Ga + Nd)-doped ZnO films with an RF magnetron (Toma et al., 2023). It was found that undoped ZnO has a resolution of 85% in the visible range. Using sol-gel dip coating method, Murthy putted thin plates of aluminum and rubidium-doped ZnO on glass surfaces (Murthy et al., 2023), and found that the quality of crystals gets worse because of lattice stress after Rb particles added to a ZnO host lattice.

3.6 PVDF piezoelectric films

There are several ways to make PVDF films, such as electrostatic spinning, solution casting, solution casting, spin coating method, electro-spinning technique, stretching, vacuum evaporation, and homogenization, etc (Jin et al., 2021; Yen et al., 2022; Das et al., 2023; Ghosh et al., 2023; Mishra et al., 2023; Sarkar et al., 2024). The scratch spraying method was used to make polyvinylidene fluoride-trifluoro ethylene (PVDF-TrFE) copolymers (Singh et al., 2018; Bhunia et al., 2019; Gupta et al., 2019; Sapkota et al., 2022). In first step, cobalt ferrite ($CoFe_2O_4$) nanoparticles were made using acoustic chemistry. In second step, cobalt ferrite nanoparticles with different weight percentages (0, 2.5, 5, and 10%) were added to PVDF-TrFE to make nanocomposites. As shown in Figure 4H, an electrostatic spinning process was employed to make polyvinylidene difluoride matrix fiber membranes with modified lead zirconate titanate nanoparticles (PZT NPs) (Yuan et al., 2023). The inserted particles changed the distribution of polarized electric field, which helped to polarize PVDF. As shown in Figure 4I, thin films substrate is made of flexible hollow fiber polymer membranes sprayed with thin layers of photocatalyst (Zakria et al., 2023). Copper oxide/polyvinylidene fluoride thin film hollow fiber membranes (Cu_xO/PVDF TF HFM) were made by spraying Cu_xO on PVDF hollow fiber membranes (HFM) with a radio frequency (RF)

magnetron. As much as 91% of the BPA was taken out of the cleaned wastewater by irradiation. After three rounds in a row, the efficiency of recycling hit about 71.3%. Flexible nanocomposite films were made by adding BFO powder to copolymers PVDF-TrFE and PVDF-HFP, showing high output voltage (Tripathy et al., 2023). Dielectric constant was reached up to 40 in an independent flexible hybrid film made of polyvinylidene fluoride (PVDF) and molybdenum disulphide (MoS_2) nanoflakes synthesized by sol-gel method, which was to be 5 times more than that of pure PVDF (Jangra et al., 2023). A lead-free, facile, low-cost, sol-gel-processed reduced graphene oxide (rGO)/P(VDF-TrFE) nanocomposite with multipurpose capability demonstration as a piezoelectric nanogenerator (PENG) and hybrid piezoelectric triboelectric nanogenerator (HPTENG) devices is presented in Ref.171. The maximum output power densities of hybrid piezo-triboelectric and piezoelectric devices are 0.28 W/cm3 and 0.34 mW/cm3, respectively. The triboelectric device demonstrates the direct illumination of 45 blue light-emitting diodes, which are connected in series to collect the mechanical energy generated by repeated finger taps (Bhunia et al., 2019).

4 Applications in self-powered IoT devices

4.1 Energy harvesting

Gathering energy from surrounding environment, like mechanical vibration, heat, fluid flow, electromagnetic radiation in form of light and radio waves (RF), and energy from body can provide clean power to run electronic devices like wireless sensor networks, mobile electronics, and wearable and implantable biomedical devices (Shirvanimoghaddam et al., 2016; Liu et al., 2018; Won et al., 2018; Ali et al., 2019). Mechanical energy is the most common type of energy that can be turned into useful power (Wang, 2012; Hu et al., 2019; Karan et al., 2019; Sun et al., 2019; Yan et al., 2019). Piezoelectric energy harvesting is a very easy way to turn mechanical energy in the environment into electrical energy. Because piezoelectric effect is based on intrinsic polarization of the material and does not need a separate voltage source, a magnetic field, or contact with another material, like electrostatic, electromagnetic, and friction electrical energy harvesting (Xie and Wang, 2015; Wang et al., 2018). Compared to other energy harvesting methods, their density output and voltage output are 3–5 times higher (Kim et al., 2011; Wu et al., 2015; Shi et al., 2018; Chen et al., 2019; Guan et al., 2020). Piezoelectric units are easy to integrate to microelectromechanical systems (Madinei et al., 2016; Zhou et al., 2020). It has been used in many fields, such as buildings, transportation, wireless electronics, MEMS, the Internet of Things (IoT), personal and internal healthcare devices (Siang et al., 2018).

Gao suggested a cantilever energy harvester using PIN-PMN-PT crystals, showing high power output with value of 102 W/m^3. The designed energy generator worked well to power wireless devices for tracking and sending data, which could help to give power supply of IoT systems in a safe way (Gao et al., 2020). As shown in Figure 5A, a droplet-based generator (DEG) for gathering energy from the natural environment has been designed (Li et al., 2022b). The self-capacitance effect of upper electrode enables an ultra-high instantaneous peak output power with value of 765 W/m^2. As shown in Figure 5B, Petritz presents an energy harvesting system used ferroelectric polymer transducers and organic diodes (Petritz et al., 2021). These components are seamlessly integrated onto ultrathin substrates with 1 μm in thickness.

The progress of CMOS has significantly contribution to self-powered direct current (DC-type) energy harvesters operating at low input voltages, enhancing the overall performance of these energy harvesters (Wang and Li, 2016). Lei presented a surface engineering approach for transparent conductive membranes using self-assembled monolayers (SAMs) in conjunction with silver nanowires (AgNWs) for triboelectric nanogenerators (TENGs) and self-powered pressure sensors (Lei et al., 2023). The enhanced.

TENG has a notable capability to function as a pressure sensor array (4 × 4 pixels) for trajectory tracking, with a high sensitivity of 221 V-kPa-1. As shown in Figure 5C, Wu developed sensors using composite thin-film infrared sensor arrays for imaging human hand (Wu et al., 2023), indicating potential use of self-powered infrared sensor in wearable non-visual sensing and smart sensing applications. As shown in Figure 5D, piezoelectric sensors were designed for real-time monitoring of meteorological wind and rain (Li et al., 2023b). The ZnO@CF/PVDF composite thin film PNG demonstrates a maximum output power of 7.9 μW under an external load of 10 MΩ. Furthermore, the remarkable washing resistance, longevity exceeding 50,000 cycles, and sustained stability over a period of 12 months make the composite film as a viable candidate for deployment of weather sensor in autonomous vehicles. Finally, self-powered physiological monitoring devices have the capability to consistently monitor and transmit electrocardiogram (ECG), blood pressure, temperature, and exercise parameters of the human body (Yan et al., 2023).

4.2 Flexible sensors

4.2.1 Bio-medical sensors

Due to the pressing demands of industry, flexible sensors have been significant investigated and focused on strain sensors for accurate motion detection, particularly in relation to human muscles (Gullapalli et al., 2010). Photodetectors designed for biomonitoring, such as continuous glucose monitoring, have experienced substantial growth in research efforts (Chung et al., 2019; Teymourian et al., 2020; Zhou et al., 2021). In addition, there is emerging interest in the advancement of temperature and humidity sensors (Park et al., 2012; Huang et al., 2013; Pandey et al., 2014; Nakajima and Tsuchiya, 2015; Fujita et al., 2016; Nakajima et al., 2017; Nakajima and Tsuchiya, 2020; Shin et al., 2020; Trudeau et al., 2020). There has been a notable surge in use of flexible gas sensors (Monereo et al., 2011; Alrammouz et al., 2018; Fioravanti and Carotta, 2020; Sugahara et al., 2020) and electrochemical sensors (Huang et al., 2011; Santos et al., 2014; Manjakkal et al., 2020) on purpose of real-time monitoring. This monitoring approach involves the analysis of human breath and sweat to effectively identify pre-symptomatic conditions with a high level of accuracy. Furthermore, flexible magnetic sensors have been extensively investigated for muscles and brain applications (Satake et al., 2019).

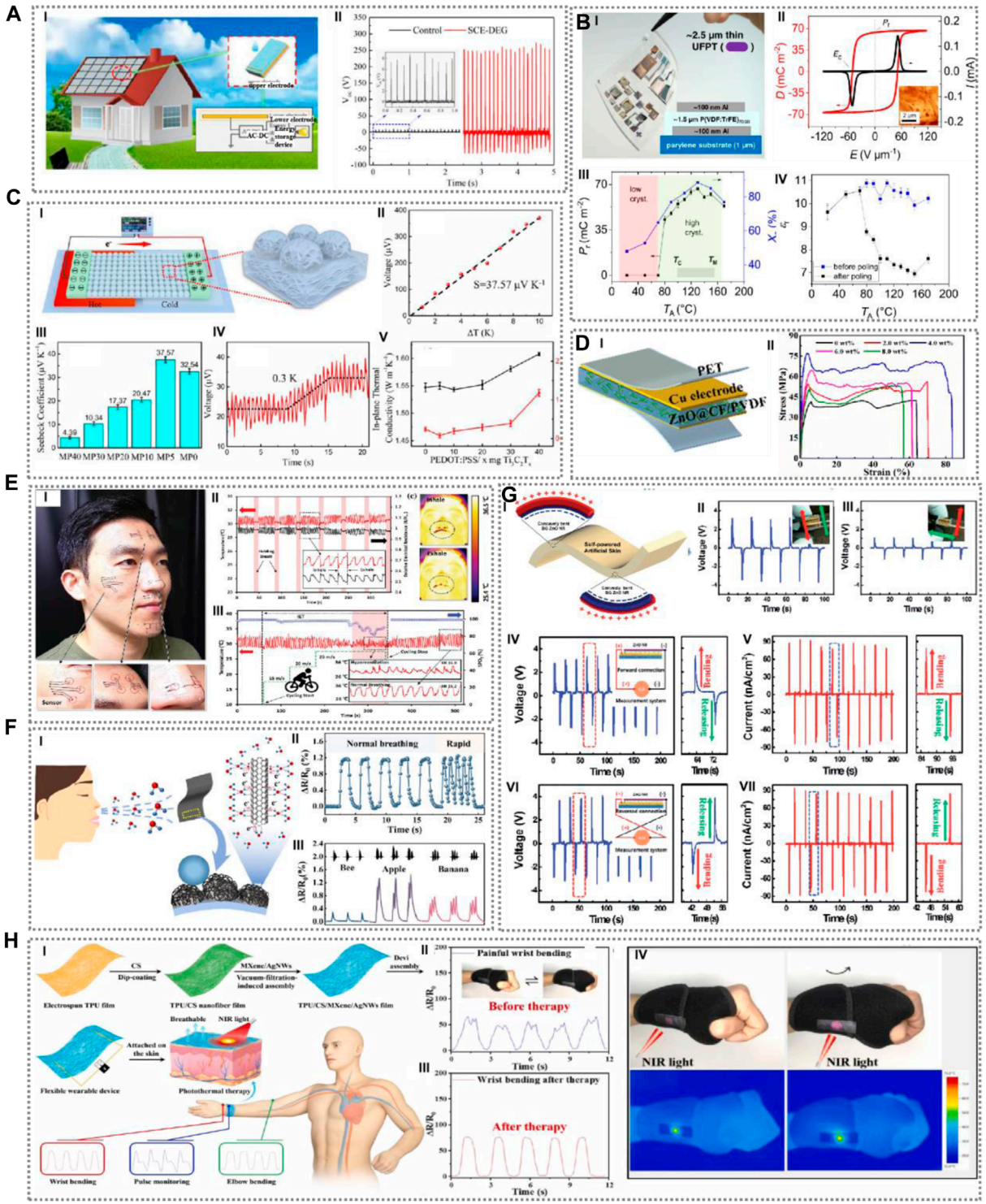

FIGURE 5
(A)-I: Application of SCE-DEG on building's roofs. **(A)**-II: Output voltage of SCE-DEG (Li et al., 2022b). **(B)**-I: Photograph of ultra-flexible P(VDF:TrFE)70:30-based transducer. **(B)**-II, III, and IV: Electrical properties of ferroelectric layers (Petritz et al., 2021). **(C)**-I: Thermoelectric conversion test system. **(C)**-II to V: Electrical properties of various PPM films (Wu et al., 2023). **(D)**-I: Structures of flexible ZnO@CF/PVDF composite films. **(D)**-II: Strain–stress curve of ZnO@CF/PVDF composite films (Li et al., 2023b). **(E)**-I: NiO epidermal temperature sensors attached at various facial positions. **(E)**-II: Continuous monitoring of breathing. **(E)**-III: Real-time monitoring of hyperventilation recorded in conjunction with SpO_2 change during incremental exercise test (Shin et al., 2020). **(F)**-I: Voiceprint and humidity signals during speaking of different volunteers. **(F)**-II: Response of sensors to different frequencies of human respiration. **(F)**-III: Voiceprint and humidity response signal of sensors in noisy environment (Sun et al., 2023). **(G)**-I: Schematic diagram of bent SPAS. **(G)**-II and III: Output voltage of BG ZnO NRs from bending parallel and vertically along rubbing direction. **(G)**-IV to VII: Output voltage and current density in devices connected in forward and reverse directions (Lee et al., 2014). **(H)**-I: Schematic fabrication of flexible breathable electronic sensor by elaborately assembling conductive MXene nanosheets and AgNWs. **(H)**-II and III: Performance of flexible breathable sensors before and after therapy. **(H)**-IV: NIR thermal images of wrist bending (Chao et al., 2023).

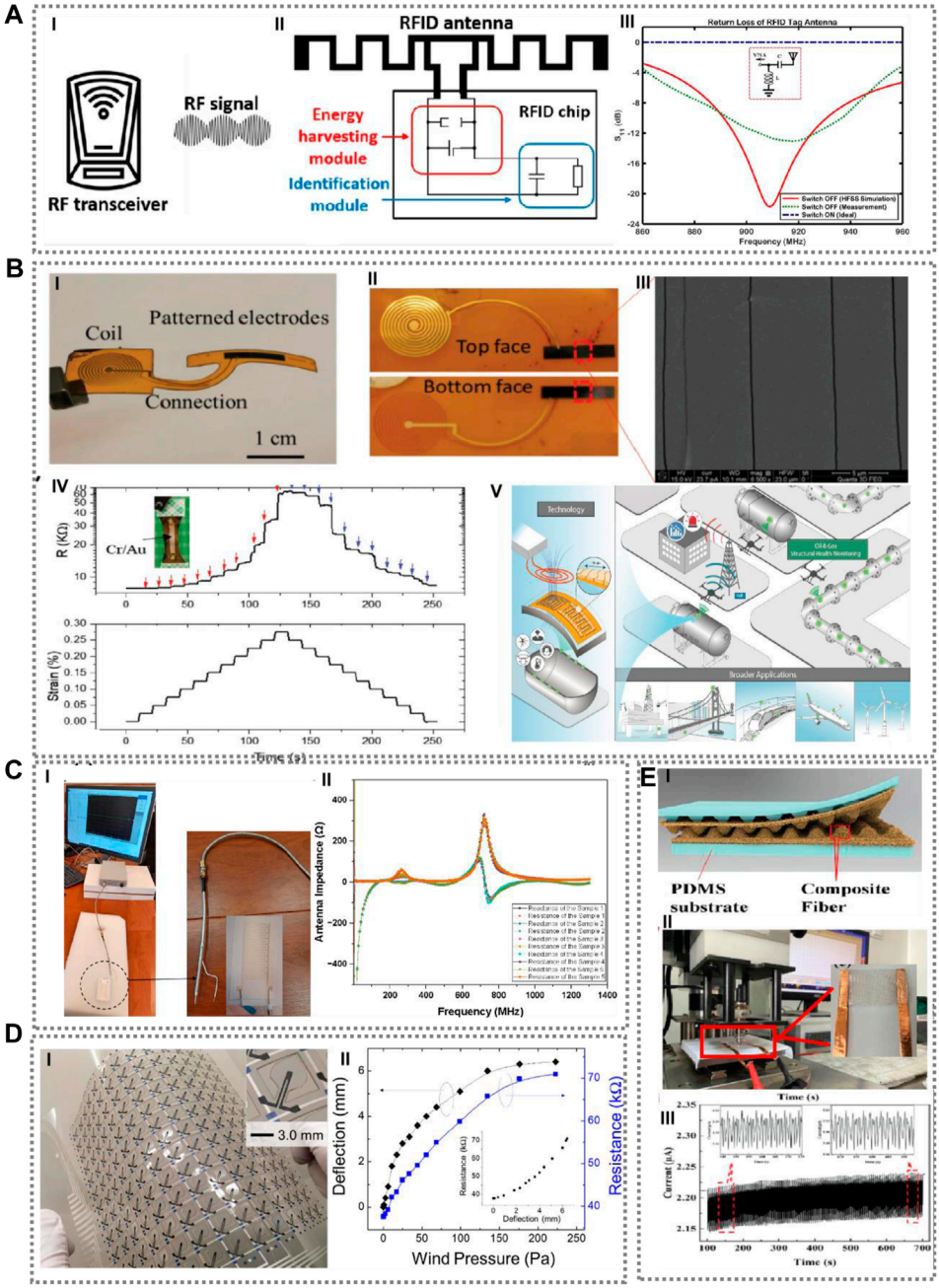

FIGURE 6
(A): Multiple smart screen-printed flexible RFID enabled self-powered sensor tags (Wang et al., 2023c). **(B)**-I and II: Photographic of designed LC sensor. **(B)**-III: SEM image of electrodes on sensors. **(B)**-IV: Resistance variation of cracked Cr/Au film under strain steps. **(B)**-V: Application of supersensitive passive RFID strain sensors (Nesser et al., 2023). **(C)**: Experimental apparatus for impedance measurement (Tekcin et al., 2022). **(D)**-I: A kind of wind pressure distribution sensor. **(D)**-II: Deflection of suspended structure and resistance recorded by single sensor for different wind pressures (Kanazawa and Ushijima, 2020). **(E)**-I and II: Micro-structures of PNG flexible composite films and experimental instrument. **(E)**-III: Current output of the devices (Lv et al., 2023b).

As shown in Figure 5E, Shin presented a novel conceptual framework for artificial skin using negative temperature coefficient (NTC) materials (Shin et al., 2020). Utilizing a network of physiological temperature sensors to evaluate the performance of temperature-sensitive artificial skin in the measurement of exhaled breath temperature, the early advancement of pathogenic conditions inside the respiratory system was identified.

On purpose of healthcare monitoring, Nakajima produced thermistor-on-a-polyimide sheet thin-film sensor arrays using strontium- and nickel-doped chalcogenide SmMnO3 (Nakajima and Tsuchiya, 2020). At bending angles of 60° and 20°, thermistor sensor exhibited notable resilience when subjected to a bending angle of 60° and a minimal bending radius of 500 μm. During a bending test including over 1,000 cycles, the observed temperature

variation remained within a narrow range of 0.1°C. Sun developed a humidity sensor with a flexible design using multi-walled carbon nanotubes (MWCNTs) that were securely affixed to the surface folds of a natural latex membrane (Sun et al., 2023), as shown in Figure 5F. The sensor has a rapid reaction time of 0.7 s and a broad humidity detection range (0%–100%) due to the weak contact link between multi-walled carbon nanotubes (MWCNTs) and water molecules. Consequently, it can effectively detect human breathing at a frequency of 1 Hz.

As shown in Figure 5G, Lee presented a cutting-edge development in the form of an ultrathin self-powered artificial skin (SPAS) that relies on the utilization of piezoelectric nanogenerators (Lee et al., 2014). The sensor is capable of gathering and storing elastic deformation energy produced as by bending and stretching movements of skin. Rim shown a novel approach including a conformal biosensor for fabrication of highly responsive field effect transistors (FETs) based on $2O_3$ (Rim et al., 2015). Ultrathin films with a thickness of 3.5 nm were fabricated, exhibiting high density and uniformity over a large surface area. Wang fabricated a flexible strain sensor by incorporating silver nanowires onto carbon black-modified electrostatically spun thermoplastic polyurethane fabric sheets, demonstrating high level of sensitivity with a strain factor over 16,000 (Wang et al., 2023b). It also possesses a wide strain range, spanning from 360.0% to 1%. Chao developed a permeable epidermal sensor by arranging conductive MXene nanosheets and silver nanowires on electrostatically spun elastic substrate (Chao et al., 2023).

As shown in Figure 5H, He presented a method for fabrication of robust nanocomposite organic hydrogel (NCO hydrogel) strain sensors and their integration into a flexible wearable device (He et al., 2023). The NCO hydrogel was affixed to substrate and linked to Bluetooth module in order to developing a portable wearable device for surveillance of human motion. Flexible sensors possess a broad spectrum of potential applications for monitoring and tracking human health in real-time (Luo et al., 2023). Nevertheless, the primary material used in flexible sensors is thin films.

4.2.2 Flexible RFID

Several challenges still need to be addressed in field of industry, particularly the design of flexible micro-nano mechanical sensors and measurement of various physical quantities such as pressure, piezoelectricity, and strain. Additionally, the synthesis of sensitive materials, conductive inks, large-area printed electronics for mass production, require further resolution.

The prevailing technology for authentication in the internet of things (IoT) is radio frequency identification (RFID). RFID is a wireless, non-contact automatic identification technology that enables the identification of specific targets, and reading and writing of relevant data through radio signals. Wang designed a detection system that utilized reeds and switch-based proximity sensors (Wang et al., 2023c). The integration of sensors with distinct passive RFID tags has been shown in Figure 6A. RFID technology can be effectively used in field of structural health monitoring (SHM), a critical aspect in guaranteeing operational safety, such as pipelines, storage tanks, aero planes, ships, and automobiles (Baumbauer et al., 2020; Nesser et al., 2023). As shown in Figure 6B, high sensitivity strain measurement data can be wireless transferred by RFID. As shown in Figure 6C, Tekcin designed a pliable sensor that relies on an inductive-capacitive (LC) circuit and a parallel-plate capacitive sensing unit (Tekcin et al., 2022). The piezoresistive properties were enhanced through the addition of tailored fractures. Lv presented a novel flexible sensor integrated pyramidal micropatterns with ion-gel nanofibers, enabling it to effectively detect both normal and tangential forces (Lv et al., 2023b). As shown in Figure 6D, Kanazawa presented a flexible sensor designed for measuring the distribution of wind pressure (Kanazawa and Ushijima, 2020). To enhance the mechanical mobility of resistive strain sensor matrix against wind, a suspension structure was integrated into a plastic sheet. The use of mechanically functionalized substrates gives an opportunity for the advancement of flexible electronics. Chen designed anisotropic magneto resistive (AMR) sensors on flexible substrates (Chen and Zhang, 2023). The AMR sensors demonstrated a maximum bending radius of around 2.3 cm under mechanical bending, illustrating the practicality of producing compact AMR sensors on flexible substrates for detecting magnetic fields in non-planar scenarios, as shown in Figure 6E.

5 Conclusion

The emergence of self-powered flexible electronic systems represents a huge paradigm shift in the future of electronics in the field of human friendliness or human integration. In particular, by capturing permanent energy and generating electricity from abundant mechanical energy, such systems are of direct interest for applications in sensor networks and wearable electronics. The rapid development of wearable devices and portable electronic systems has raised the demand for transferable, adaptable, wearable, flexible, mechanically robust and stable energy sources that can provide the required power from renewable sources. In this work, we highlight the latest advances and achievements in field of piezoelectric thin film used as self-powered sensors. Firstly, piezoelectric energy conversion materials are the core of sensor function. Crystalline structure, morphology and electrical properties in several kinds of piezoelectric thin films, especially high-performance lead-based films, lead free films, and biofilms, are reviewed. In addition, piezoelectric properties of films doped with various elements are summarized and the corresponding synthesis processes are analyzed. Second, manufacturing process of thin film sensors is outlined, followed by a brief overview of techniques used in microelectromechanical system (MEMS) processing. Furthermore, industrial practices regarding batch fabrication of MEMS are analyzed. Thirdly, the application scenarios of latest thin film sensors used in internet of things are introduced, including energy harvesting, biosensors, RF sensors, et al. It highlights the significant performance improvements presented by these advanced thin film sensors in different application areas. Finally, the existing thin film technique is subject to several restrictions, including challenges in industrial preparation and processing, as well as issues related to dimensional accuracy, among others. Future research should consider improving film quality and developing ecologically sustainable film production methods. Piezoelectric self-powered nanogenerators can be used in wearable electronic products,

medical devices, automotive sensors, and wireless sensor monitoring systems without affecting the environment. This review is aimed at guiding the next-generation to pay more attention to piezoelectric flexibility sensors.

Author contributions

ZS: Conceptualization, Writing–original draft, Writing–review and editing. RH: Investigation, Visualization, Writing–review and editing. FJ: Conceptualization, Formal Analysis, Resources, Validation, Writing–original draft.

Funding

The author(s) declare that financial support was received for the research, authorship, and/or publication of this article. This work was funded by Major Project of Colleges and Universities Natural Science Foundation in Jiangsu Province (21KJA470003) and Wuxi University Research Start-up Fund for Introduced Talents (2021r001, 2023r022).

Conflict of interest

The authors declare that the research was conducted in the absence of any commercial or financial relationships that could be construed as a potential conflict of interest.

Publisher's note

All claims expressed in this article are solely those of the authors and do not necessarily represent those of their affiliated organizations, or those of the publisher, the editors and the reviewers. Any product that may be evaluated in this article, or claim that may be made by its manufacturer, is not guaranteed or endorsed by the publisher.

References

Abdullah, A. M., Sadaf, M. U. K., Tasnim, F., Vasquez, H., Lozano, K., and Uddin, M. J. (2021). KNN based piezo-triboelectric lead-free hybrid energy films. *Nano Energy* 86, 106133. doi:10.1016/j.nanoen.2021.106133

Agarwala, S., Goh, G. L., Yap, Y. L., Goh, G. D., Yu, H., Yeong, W. Y., et al. (2017). Development of bendable strain sensor with embedded microchannels using 3D printing. *Sensors Actuators A Phys.* 263, 593–599. doi:10.1016/j.sna.2017.07.025

Akiyama, M., Kamohara, T., Kano, K., Teshigahara, A., Takeuchi, Y., and Kawahara, N. (2009b). Enhancement of piezoelectric response in scandium aluminum nitride alloy thin films prepared by dual reactive cosputtering. *Adv. Mat.* 21 (5), 593–596. doi:10.1002/adma.200802611

Akiyama, M., Kano, K., and Teshigahara, A. (2009a). Influence of growth temperature and scandium concentration on piezoelectric response of scandium aluminum nitride alloy thin films. *Appl. Phys. Lett.* 95 (16), 162107. doi:10.1063/1.3251072

Akmal, M. H. M., Warikh, A. R. M., Azlan, U. A. A., Azmi, N. A., Salleh, M. S., and Kasim, M. S. (2018). Optimizing the processing conditions of sodium potassium niobate thin films prepared by sol-gel spin coating technique. *Ceram. Int.* 44 (1), 317–325. doi:10.1016/j.ceramint.2017.09.175

Algün, G., Akçay, N., Öztel, H. O., and Can, M. M. (2023). Synthesis and ultrafast humidity sensing performance of Sr doped ZnO nanostructured thin films: the effect of Sr concentration. *J. Sol-Gel Sci. Technol.* 107 (3), 640–658. doi:10.1007/s10971-023-06148-0

Ali, F., Raza, W., Li, X., Gul, H., and Kim, K.-H. (2019). Piezoelectric energy harvesters for biomedical applications. *Nano Energy* 57, 879–902. doi:10.1016/j.nanoen.2019.01.012

Alrammouz, R., Podlecki, J., Abboud, P., Sorli, B., and Habchi, R. (2018). A review on flexible gas sensors: from materials to devices. *Sensors Actuators A Phys.* 284, 209–231. doi:10.1016/j.sna.2018.10.036

Antony Jeyaseelan, A., and Dutta, S. (2020). Improvement in piezoelectric properties of PLZT thin film with large cation doping at A-site. *J. Alloys Compd.* 826, 153956. doi:10.1016/j.jallcom.2020.153956

Aratani, M., Oikawa, T., Ozeki, T., and Funakubo, H. (2001). Epitaxial-grade polycrystalline Pb(Zr,Ti)O3 film deposited at low temperature by pulsed-metalorganic chemical vapor deposition. *Appl. Phys. Lett.* 79 (7), 1000–1002. doi:10.1063/1.1391229

Atlam, H. F., Walters, R. J., and Wills, G. B. (2018). Internet of things: state-of-the-art, challenges, applications, and open issues. *J. Netw. Comput. Appl.* 67, 99–117. doi:10.1016/j.jnca.2016.01.010

Bagchi, B., Hoque, N. A., Janowicz, N., Das, S., and Tiwari, M. K. (2020). Re-useable self-poled piezoelectric/piezocatalytic films with exceptional energy harvesting and water remediation capability. *Nano Energy* 78, 105339. doi:10.1016/j.nanoen.2020.105339

Bai, L., Zhu, K., Qiu, J., Zhu, R., Gu, H., and Ji, H. (2011). Synthesis of (K,Na)NbO3 particles by traditional hydrothermal method and high-temperature mixing method under hydrothermal–solvothermal conditions. *Res. Chem. Intermed.* 37 (2), 185–193. doi:10.1007/s11164-011-0265-3

Baumbauer, C. L., Anderson, M. G., Ting, J., Sreekumar, A., Rabaey, J. M., Arias, A. C., et al. (2020). Printed, flexible, compact UHF-RFID sensor tags enabled by hybrid electronics. *Sci. Rep.* 10 (1), 16543. doi:10.1038/s41598-020-73471-9

Beklešovas, B., Iljinas, A., Stankus, V., Čyvienė, J., Andrulevičius, M., Ivanov, M., et al. (2022). Structural, morphologic, and ferroelectric properties of PZT films deposited through layer-by-layer reactive DC magnetron sputtering. *Coatings* 12 (6), 717. doi:10.3390/coatings12060717

Bhunia, R., Gupta, S., Fatma, B., Gupta, R. K., and Garg, A. (2019). Milli-watt power harvesting from dual triboelectric and piezoelectric effects of multifunctional green and robust reduced graphene oxide/P(VDF-TrFE) composite flexible films. *ACS Appl. Mater. Interfaces* 11, 38177–38189. doi:10.1021/acsami.9b13360

Bian, K., Gu, Q., Zhu, K., Zhu, R., Wang, J., Liu, J., et al. (2016). Improved sintering activity and piezoelectric properties of PZT ceramics from hydrothermally synthesized powders with Pb excess. *J. Mater. Sci. Mater. Electron.* 27 (8), 8573–8579. doi:10.1007/s10854-016-4875-9

Biswas, P., Hoque, N. A., Thakur, P., Saikh, M. M., Roy, S., Khatun, F., et al. (2019). Highly efficient and durable piezoelectric nanogenerator and photo-power cell based on CTAB modified montmorillonite incorporated PVDF film. *ACS Sustain. Chem. Eng.* 7, 4801–4813. doi:10.1021/acssuschemeng.8b05080

Botta, A., Donato, Wd, Persico, V., and Ajfgcs, P. (2016). Integration of cloud computing and internet of things: a survey. *Future Gener. Comput. Syst.* 56, 684–700. doi:10.1016/j.future.2015.09.021

Bouad, V., Fadel, A., Mohan, S., Hamieh, A., Tahon, J.-F., Lyskawa, J., et al. (2022). Utilization of catechol end-functionalized PMMA as a macromolecular coupling agent for ceramic/fluoropolymer piezoelectric composites. *ACS Appl. Polym. Mater.* 4 (10), 7258–7267. doi:10.1021/acsapm.2c00883

Chao, M., Di, P., Yuan, Y., Xu, Y., Zhang, L., and Wan, P. (2023). Flexible breathable photothermal-therapy epidermic sensor with MXene for ultrasensitive wearable human-machine interaction. *Nano Energy* 108, 108201. doi:10.1016/j.nanoen.2023.108201

Chen, J., Oh, S. K., Nabulsi, N., Johnson, H., Wang, W., and Ryou, J.-H. (2019). Biocompatible and sustainable power supply for self-powered wearable and implantable electronics using III-nitride thin-film-based flexible piezoelectric generator. *Nano Energy* 57, 670–679. doi:10.1016/j.nanoen.2018.12.080

Chen, J., and Zhang, Z. (2023). A flexible anisotropic magnetoresistance sensor for magnetic field detection. *J. Mater. Sci. Mater. Electron.* 34 (1), 73. doi:10.1007/s10854-022-09400-5

Chen, K., Gao, W., Emaminejad, S., Kiriya, D., Ota, H., Nyein, H. Y. Y., et al. (2016). Printed carbon nanotube electronics and sensor systems. *Adv. Mat.* 28 (22), 4397–4414. doi:10.1002/adma.201504958

Chen, S., Zhu, P., Mao, L., Wu, W., Lin, H., Xu, D., et al. (2023a). Piezocatalytic medicine: an emerging frontier using piezoelectric materials for biomedical applications. *Adv. Mat.* 35 (25), 2208256. doi:10.1002/adma.202208256

Chen, X., Sun, J., Guo, B., Wang, Y., Yu, S., Wang, W., et al. (2022). Effect of the particle size on the performance of BaTiO3 piezoelectric ceramics produced by additive manufacturing. *Ceram. Int.* 48 (1), 1285–1292. doi:10.1016/j.ceramint.2021.09.213

Chen, Z., Hao, Y., Huang, J., Zhou, Z., Li, Y., and Liang, R. (2023b). Poling above the Curie temperature driven large enhancement in piezoelectric performance of Mn doped PZT-based piezoceramics. *Nano Energy* 113, 108546. doi:10.1016/j.nanoen.2023.108546

Cheng, Y., Fan, W., Chen, H., Xie, L., Xing, J., Tan, Z., et al. (2022). Hardening effect in lead-free KNN-based piezoelectric ceramics with CuO doping. *ACS Appl. Mater. Interfaces* 14 (50), 55803–55811. doi:10.1021/acsami.2c18015

Chionh, C. Y., Soh, D. Y., Tan, C. H., Khaw, J. Y., Wong, Y. C., Roy, D. M., et al. (2020). A device for surveillance of vascular access sites for bleeding: results from a clinical evaluation trial. *Sci. Rep.* 23, 18153. doi:10.1038/s41598-020-74571-2

Choi, S., Lee, H., Ghaffari, R., Hyeon, T., and Kim, D.-H. (2016). Recent advances in flexible and stretchable bio-electronic devices integrated with nanomaterials. *Adv. Mat.* 28 (22), 4203–4218. doi:10.1002/adma.201504150

Chorsi, M. T., Curry, E. J., Chorsi, H. T., Das, R., Baroody, J., Purohit, P. K., et al. (2019). Piezoelectric biomaterials for sensors and actuators. *Adv. Mat.* 31 (1), 1802084. doi:10.1002/adma.201802084

Chortos, A., Liu, J., and Bao, Z. (2016). Pursuing prosthetic electronic skin. *Nat. Mater.* 15 (9), 937–950. doi:10.1038/nmat4671

Chung, M., Fortunato, G., and Radacsi, N. (2019). Wearable flexible sweat sensors for healthcare monitoring: a review. *J. R. Soc. Interface.* 16 (159), 20190217. doi:10.1098/rsif.2019.0217

Cuadra, J. G., Estrada, A. C., Oliveira, C., Abderrahim, L. A., Porcar, S., Fraga, D., et al. (2023). Functional properties of transparent ZnO thin films synthetized by using spray pyrolysis for environmental and biomedical applications. *Ceram. Int.* 49 (20), 32779–32788. doi:10.1016/j.ceramint.2023.07.246

Cui, Y., Liu, F., Jing, X., and Mu, J. (2021). Integrating sensing and communications for ubiquitous IoT: applications, trends, and challenges. *IEEE Netw.* 35, 158–167. doi:10.1109/mnet.010.2100152

Das, N., Sarkar, D., Saikh, M. M., Biswas, P., Das, S., Hoque, N. A., et al. (2022). Piezoelectric activity assessment of size-dependent naturally acquired mud volcano clay nanoparticles assisted highly pressure sensitive nanogenerator for green mechanical energy harvesting and body motion sensing. *Nano Energy* 102, 107628. doi:10.1016/j.nanoen.2022.107628

Das, N., Sarkar, D., Yadav, N., Ali, A., Das, S., Pratim Ray, P., et al. (2023). Development of a lead-free, high-frequency ultrasound transducer with broad bandwidth and enhanced pulse-echo response, employing β-Ni(OH)2/PVDF-TrFE piezoelectric composite. *Chem. Eng. J.* 475, 146322. doi:10.1016/j.cej.2023.146322

Das, S., Biswal, A. K., and Roy, A. (2017). Fabrication of flexible piezoelectric PMN-PT based composite films for energy harvesting. *IOP Conf. Ser. Mater. Sci. Eng.* 178 (1), 012020. doi:10.1088/1757-899x/178/1/012020

Das, S., Biswal, A. K., Parida, K., Choudhary, R. N. P., and Roy, A.(2018). Electrical and mechanical behavior of PMN-PT/CNT based polymer composite film for energy harvesting. *Appl. Surf. Sci.* 428, 356–363. doi:10.1016/j.apsusc.2017.09.077

Debeuckelaere, K., Janssens, D., Asensio, E. S., Wenseleers, T., Jacquemyn, H., and Pozo, M. I. (2023). A wireless, user-friendly, and unattended robotic flower system to assess pollinator foraging behaviour. *biorxiv*. doi:10.1101/2022.06.14.496104

Dhanumalayan, E., and Joshi, G. M. (2018). Performance properties and applications of polytetrafluoroethylene (PTFE)—a review. *Adv. Compos. Hybrid Mater.* 1 (2), 247–268. doi:10.1007/s42114-018-0023-8

Di Marco, M. B., Imhoff, L., Roldán, M. V., Barolin, S., and Stachiotti, M. G. (2023). Sol–gel synthesis and characterization of PZT thin films on FTO/aluminoborosilicate glass substrates. *J. Mater. Sci. Mater. Electron.* 34 (14), 1171. doi:10.1007/s10854-023-10596-3

Dong, W., Sun, Y., Wang, B., Zhu, M., Li, J., Xu, X., et al. (2022). Bi3TeBO9: a borate piezoelectric crystal with a high piezoelectric coefficient. *Cryst. Growth and Des.* 22 (7), 4243–4249. doi:10.1021/acs.cgd.2c00260

Eini, R., Linkous, L., Zohrabi, N., and Abdelwahed, S. J. (2021). Smart building management system: performance specifications and design requirements. *J. Build. Eng.* 39, 102222. doi:10.1016/j.jobe.2021.102222

Fakhri, P., Amini, B., Bagherzadeh, R., Kashfi, M., Latifi, M., Yavari, N., et al. (2019). Flexible hybrid structure piezoelectric nanogenerator based on ZnO nanorod/PVDF nanofibers with improved output. *RSC Adv.* 9 (18), 10117–10123. doi:10.1039/c8ra10315a

Fan, Z., Qian, C., Jia, Y., Wang, Z., Ding, Y., Wang, D., et al. (2022). Homeostatic neuro-metasurfaces for dynamic wireless channel management. *Sci. Adv.* 8 (27), eabn7905. doi:10.1126/sciadv.abn7905

Fast, D., Clark, M., Fullmer, L., Grove, K., Nyman, M., Gibbons, B., et al. (2020). Using simple aqueous precursors for a green synthetic pathway to potassium sodium niobate thin films. *Thin Solid Films* 710, 138270. doi:10.1016/j.tsf.2020.138270

Fei, C., Liu, X., Zhu, B., Li, D., Yang, X., Yang, Y., et al. (2018). AlN piezoelectric thin films for energy harvesting and acoustic devices. *Nano Energy* 51, 146–161. doi:10.1016/j.nanoen.2018.06.062

Feng, G.-H., Li, C.-Y., Chen, Y.-H., Ho, Y.-C., Chu, S.-Y., Tsai, C.-C., et al. (2022). Investigation of Mo doping effects on the properties of AlN-based piezoelectric films using a sputtering technique. *ECS J. Solid State Sci. Technol.* 11 (12), 123005. doi:10.1149/2162-8777/aca796

Fiedler, H., Leveneur, J., Mitchell, D. R. G., Arulkumaran, S., Ng, G. I., Alphones, A., et al. (2021). Enhancing the piezoelectric modulus of wurtzite AlN by ion beam strain engineering. *Appl. Phys. Lett.* 118 (1). doi:10.1063/5.0031047

Fioravanti, A., and Carotta, M. C. (2020). Year 2020: a snapshot of the last progress in flexible printed gas sensors. *Appl. Sci.* 10 (5), 1741. doi:10.3390/app10051741

Fujita, T., Tanaka, H., Inaba, H., and Nagatomo, N. (2016). Development and electrical properties of wurtzite (Al,Ti)N materials for thin film thermistors. *J. Ceram. Soc. Jpn.* 124, 653–658. doi:10.2109/jcersj2.15316

Gao, X., Qiu, C., Li, G., Ma, M., Yang, S., Xu, Z., et al. (2020). High output power density of a shear-mode piezoelectric energy harvester based on $Pb(In_{1/2}Nb_{1/2})O_3$-$Pb(Mg_{1/3}Nb_{2/3})O_3$-$PbTiO_3$ single crystals. *Appl. Energy* 271, 115193. doi:10.1016/j.apenergy.2020.115193

Gatabi, J. R., Rahman, S., Amaro, A., Nash, T., Rojas-Ramirez, J., Pandey, R. K., et al. (2017). Tuning electrical properties of PZT film deposited by Pulsed Laser Deposition. *Ceram. Int.* 43 (8), 6008–6012. doi:10.1016/j.ceramint.2017.01.139

Ge, J., Sun, L., Zhang, F.-R., Zhang, Y., Shi, L.-A., Zhao, H.-Y., et al. (2016). A stretchable electronic fabric artificial skin with pressure-lateral strain-and flexion-sensitive properties. *Adv. Mat.* 28 (4), 722–728. doi:10.1002/adma.201504239

Ghosh, S., Bardhan, S., Mondal, D., Sarkar, D., Roy, J., Roy, S., et al. (2023). Natural hematite-based self-poled piezo-responsive membrane for harvesting energy from water flow and catalytic removal of organic dye. *Ceram. Int.* 49, 14710–14718. doi:10.1016/j.ceramint.2023.01.067

Guan, X., Xu, B., and Gong, J. (2020). Hierarchically architected polydopamine modified BaTiO3@P(VDF-TrFE) nanocomposite fiber mats for flexible piezoelectric nanogenerators and self-powered sensors. *Nano Energy* 70, 104516. doi:10.1016/j.nanoen.2020.104516

Guan, Y., Bai, M., Li, Q., Li, W., Liu, G., Liu, C., et al. (2022). A plantar wearable pressure sensor based on hybrid lead zirconate-titanate/microfibrillated cellulose piezoelectric composite films for human health monitoring. *Lab a Chip* 22 (12), 2376–2391. doi:10.1039/d2lc00051b

Gullapalli, H., Vemuru, V. S. M., Kumar, A., Botello-Mendez, A., Vajtai, R., Terrones, M., et al. (2010). Flexible piezoelectric ZnO–paper nanocomposite strain sensor. *Small* 6 (15), 1641–1646. doi:10.1002/smll.201000254

Gupta, S., Bhunia, R., Fatma, B., Maurya, D., Singh, D., Gupta, R., et al. (2019). Multifunctional and flexible polymeric nanocomposite films with improved ferroelectric and piezoelectric properties for energy generation devices. *ACS Appl. Energy Mater.* 2, 6364–6374. doi:10.1021/acsaem.9b01000

Habeeb Khan, A. M., Prabu, M., Khan, A. K., and Sreeja, T. K. (2023). Dielectric and ferroelectric characterization of niobium doped pzt (52/48) nanoceramics. *J. Alloys Compd.* 967, 171529. doi:10.1016/j.jallcom.2023.171529

Hao, J., Li, W., Zhai, J., and Chen, H. (2019). Progress in high-strain perovskite piezoelectric ceramics. *Mater. Sci. Eng. R Rep.* 135, 1–57. doi:10.1016/j.mser.2018.08.001

Hasan, Z., Rahman, M. A., Das, D. K., and Rouf, H. K. (2023). Influence of Ca doping in structural, electronic, optical and mechanical properties of Ba1−xCaxTiO3 perovskite from first-principles investigation. *Sci. Rep.* 13 (1), 10487. doi:10.1038/s41598-023-36719-8

He, Z., Hua, H., Zou, Z., Shu, L., Wang, T., Sun, W., et al. (2023). A facilely prepared notch-insensitive nanocomposite organohydrogel-based flexible wearable device for long-term outdoor human motion monitoring and recognition. *J. Mater. Chem. C* 11 (6), 2316–2327. doi:10.1039/d2tc05038b

Hema Malini, V., B, I., Gunasekhar, R., and Anand Prabu, A. (2022). A review on electrospun PVDF-doped metal oxide nanoparticles for sensor applications. *ECS Trans.* 107 (1), 14675–14685. doi:10.1149/10701.14675ecst

Hinchet, R., Khan, U., Falconi, C., and Kim, S.-W. (2018). Piezoelectric properties in two-dimensional materials: simulations and experiments. *Mater. Today* 21 (6), 611–630. doi:10.1016/j.mattod.2018.01.031

Hoque, N. A., Thakur, P., Biswas, P., Saikh, M. M., Roy, S., Bagchi, B., et al. (2018). Biowaste crab shell-extracted chitin nanofiber-based superior piezoelectric nanogenerator. *J. Mater. Chem. A* 6, 13848–13858. doi:10.1039/C8TA04074E

Hoque, N. A., Thakur, P., Roy, S., Kool, A., Bagchi, B., Biswas, P., et al. (2017). Er3+/Fe3+ stimulated electroactive, visible light emitting, and high dielectric flexible PVDF film based piezoelectric nanogenerators: a simple and superior self-powered energy harvester with remarkable power density. *ACS Appl. Mater. Interfaces* 9, 23048–23059. doi:10.1021/acsami.7b08008

Hu, D., Yao, M., Fan, Y., Ma, C., Fan, M., and Liu, M. (2019). Strategies to achieve high performance piezoelectric nanogenerators. *Nano Energy* 55, 288–304. doi:10.1016/j.nanoen.2018.10.053

Hu, X., Tai, Z., and Yang, C. (2018). Preparation and characterization of Er-doped AlN films by RF magnetron sputtering. *Mater. Lett.* 217, 281–283. doi:10.1016/j.matlet.2017.12.111

Huang, C.-C., Kao, Z.-K., and Liao, Y.-C. (2013). Flexible miniaturized nickel oxide thermistor arrays via inkjet printing technology. *ACS Appl. Mater. interfaces* 5 (24), 12954–12959. doi:10.1021/am404872j

Huang, W.-D., Cao, H., Deb, S., Chiao, M., and Chiao, J. C. (2011). A flexible pH sensor based on the iridium oxide sensing film. *Sensors Actuators A Phys.* 169 (1), 1–11. doi:10.1016/j.sna.2011.05.016

Huang, Y., Rui, G., Li, Q., Allahyarov, E., Li, R., Fukuto, M., et al. (2021). Enhanced piezoelectricity from highly polarizable oriented amorphous fractions in biaxially oriented poly(vinylidene fluoride) with pure β crystals. *Nat. Commun.* 12 (1), 675. doi:10.1038/s41467-020-20662-7

Huang, Z., Li, L., Wu, T., Xue, T., Sun, W., Pan, Q., et al. (2023). Wearable perovskite solar cells by aligned liquid crystal elastomers. *Nat. Commun.* 14, 1204. doi:10.1038/s41467-023-36938-7

Hwang, S.-W., Lee, C. H., Cheng, H., Jeong, J.-W., Kang, S.-K., Kim, J.-H., et al. (2015). Biodegradable elastomers and silicon nanomembranes/nanoribbons for stretchable, transient electronics, and biosensors. *Nano Lett.* 15 (5), 2801–2808. doi:10.1021/nl503997m

Jangra, M., Thakur, A., Dam, S., Chatterjee, S., and Hussain, S. (2023). Enhanced dielectric properties of MoS2/PVDF free-standing, flexible films for energy harvesting applications. *Mater. Today Commun.* 34, 105109. doi:10.1016/j.mtcomm.2022.105109

Jin, Z., Lei, D., Wang, Y., Wu, L., and Hu, N. (2021). Influences of poling temperature and elongation ratio on PVDF-HFP piezoelectric films. *Nanotechnol. Rev.* 10 (1), 1009–1017. doi:10.1515/ntrev-2021-0070

Joseph, J., Singh, S. G., and Vanjari, S. R. K. (2018). Piezoelectric micromachined ultrasonic transducer using silk piezoelectric thin film. *IEEE Electron Device Lett.* 39 (5), 749–752. doi:10.1109/led.2018.2816646

Kahveci, O., Akkaya, A., Yücel, E., Aydın, R., and Şahin, B. (2023). Production of p-CuO/n-ZnO:Co nanocomposite heterostructure thin films: an optoelectronic study. *Ceram. Int.* 49 (10), 16458–16466. doi:10.1016/j.ceramint.2023.02.007

Kalyanasundaram Balasubramanian, K., Foster, N., Zini, G., Cavallo, A., Becchio, C., et al. (2023). Neural network-based Bluetooth synchronization of multiple wearable devices. *Nat. Commun.* 14, 4472. doi:10.1038/s41467-023-40114-2

Kanazawa, S., and Ushijima, H. (2020). Development of a strain sensor matrix on mobilized flexible substrate for the imaging of wind pressure distribution. *Micromachines* 11 (2), 232. doi:10.3390/mi11020232

Kar, E., Bose, N., Dutta, B., Banerjee, S., Mukherjee, N., and Mukherjee, S. (2019). 2D SnO2 nanosheet/PVDF composite based flexible, self-cleaning piezoelectric energy harvester. *Energy Convers. Manag.* 184, 600–608. doi:10.1016/j.enconman.2019.01.073

Karan, S. K., Maiti, S., Agrawal, A. K., Das, A. K., Maitra, A., Paria, S., et al. (2019). Designing high energy conversion efficient bio-inspired vitamin assisted single-structured based self-powered piezoelectric/wind/acoustic multi-energy harvester with remarkable power density. *Nano Energy* 59, 169–183. doi:10.1016/j.nanoen.2019.02.031

Karvounis, A., Timpu, F., Vogler-Neuling, V. V., Savo, R., and Grange, R. (2020). Barium titanate nanostructures and thin films for photonics. *Adv. Opt. Mat.* 8 (24), 2001249. doi:10.1002/adom.202001249

Khan, F., Kowalchik, T., Roundy, S., and Warren, R. (2021). Stretching-induced phase transitions in barium titanate-poly(vinylidene fluoride) flexible composite piezoelectric films. *Scr. Mater.* 193, 64–70. doi:10.1016/j.scriptamat.2020.10.036

Khorrami, G. H., Mousavi, M., and Dowran, M. (2017). Structural and optical properties of KNN nanoparticles synthesized by a sol–gel combustion method. *Mod. Phys. Lett. B* 31 (15), 1750175. doi:10.1142/s0217984917501755

Kim, D., Han, S. A., Kim, J. H., Lee, J.-H., Kim, S.-W., and Lee, S.-W. (2020). Biomolecular piezoelectric materials: from amino acids to living tissues. *Adv. Mat.* 32 (14), 1906989. doi:10.1002/adma.201906989

Kim, H. S., Kim, J.-H., and Kim, J. (2011). A review of piezoelectric energy harvesting based on vibration. *Int. J. Precis. Eng. Manuf.* 12 (6), 1129–1141. doi:10.1007/s12541-011-0151-3

Kim, M., Wu, Y. S., Kan, E. C., and Fan, J. (2018). Breathable and flexible piezoelectric ZnO@PVDF fibrous nanogenerator for wearable applications. *Polymers* 10, 745. doi:10.3390/polym10070745

Kirthika, S. K., Ponraj, G., and Ren, H. (2017). Fabrication and comparative study on sensing characteristics of soft textile-layered tactile sensors. *IEEE Sensors Lett.* 1 (3), 1–4. doi:10.1109/lsens.2017.2708425

Koh, D., Ko, S. W., Yang, J. I., Akkopru-Akgun, B., and Trolier-McKinstry, S. (2022). Effect of Mg-doping and Fe-doping in lead zirconate titanate (PZT) thin films on electrical reliability. *J. Appl. Phys.* 132 (17). doi:10.1063/5.0101308

Koseki, Y., Aimi, K., and Ando, S. (2012). Crystalline structure and molecular mobility of PVDF chains in PVDF/PMMA blend films analyzed by solid-state 19F MAS NMR spectroscopy. *Polym. J.* 44 (8), 757–763. doi:10.1038/pj.2012.76

Kovacova, V., Yang, J. I., Jacques, L., Ko, S. W., Zhu, W., and Trolier-McKinstry, S. (2020). Comparative solution synthesis of Mn doped (Na,K)NbO3 thin films. *Chem. - A Eur. J.* 26 (42), 9356–9364. doi:10.1002/chem.202000537

Kumar, A., De, P. S., and Roy, A. (2023). Revisiting lead magnesium niobate-lead titanate piezoceramics for low-frequency mechanical vibration-based energy harvesting. *J. Alloys Compd.* 945, 169298. doi:10.1016/j.jallcom.2023.169298

Lay, R., Deijs, G. S., and Malmström, J. (2021). The intrinsic piezoelectric properties of materials – a review with a focus on biological materials. *RSC Adv.* 11 (49), 30657–30673. doi:10.1039/d1ra03557f

Lee, T. I., Jang, W. S., Lee, E., Kim, Y. S., Wang, Z. L., Baik, H. K., et al. (2014). Ultrathin self-powered artificial skin. *Energy and Environ. Sci.* 7 (12), 3994–3999. doi:10.1039/c4ee02358g

Lee, Y.-C., Tsai, C.-C., Liou, Y.-C., Hong, C.-S., and Chu, S.-Y. (2021). Effects of Nb doping on crystalline orientation, microstructure and electrical properties of non-stoichiometric PZT thick films via hybrid sol-gel method. *ECS J. Solid State Sci. Technol.* 10 (6), 063010. doi:10.1149/2162-8777/ac0a40

Lei, Y., Yang, J., Xiong, Y., Wu, S., Guo, W., Liu, G.-S., et al. (2023). Surface engineering AgNW transparent conductive films for triboelectric nanogenerator and self-powered pressure sensor. *Chem. Eng. J.* 462, 142170. doi:10.1016/j.cej.2023.142170

Le Rhun, G., Pavageau, F., Wagué, B., Perreau, P., Licitra, C., Frey, L., et al. (2022). Highly transparent PZT capacitors on glass obtained by layer transfer process. *J. Mater. Sci. Mater. Electron.* 33 (36), 26825–26833. doi:10.1007/s10854-022-09347-7

Li, F., Cabral, M. J., Xu, B., Cheng, Z., Dickey, E. C., LeBeau, J. M., et al. (2019). Giant piezoelectricity of Sm-doped $Pb(Mg_{1/3}Nb_{2/3})O_3$-$PbTiO_3$ single crystals. *Science* 364 (6437), 264–268. doi:10.1126/science.aaw2781

Li, H., Hu, Y., Wei, S., Meng, Y., Wang, N., Zhang, Q., et al. (2023a). Oxygen plasma-assisted ultra-low temperature sol-gel-preparation of the PZT thin films. *Ceram. Int.* 49 (7), 10864–10870. doi:10.1016/j.ceramint.2022.11.279

Li, S., Zhao, X., Bai, Y., Li, Y., Ai, C., and Wen, D. (2018). Fabrication technology and characteristics research of the acceleration sensor based on Li-doped ZnO piezoelectric thin films. *Micromachines* 9 (4), 178. doi:10.3390/mi9040178

Li, W., Sun, X., Wen, C., Lu, H., and Wang, Z. (2013). Preparation and characterization of poly (vinylidene fluoride)/TiO2 hybrid membranes. *Front. Environ. Sci. Eng.* 7 (4), 492–502. doi:10.1007/s11783-012-0407-x

Li, Y., Hu, Q., Zhang, R., Ma, W., Pan, S., Zhao, Y., et al. (2022a). Piezoelectric nanogenerator based on electrospinning PVDF/cellulose acetate composite membranes for energy harvesting. *Materials* 15, 7026. doi:10.3390/ma15197026

Li, Y., Sun, J., Li, P., Li, X., Tan, J., Zhang, H., et al. (2023b). High-performance piezoelectric nanogenerators based on hierarchical ZnO@CF/PVDF composite film for self-powered meteorological sensor. *J. Mater. Chem. A* 11 (25), 13708–13719. doi:10.1039/d3ta01886e

Li, Z., Yang, D., Zhang, Z., Lin, S., Cao, B., Wang, L., et al. (2022b). A droplet-based electricity generator for large-scale raindrop energy harvesting. *Nano Energy* 100, 107443. doi:10.1016/j.nanoen.2022.107443

Liao, C., Zhang, M., Yao, M. Y., Hua, T., Li, L., and Yan, F. (2015). Flexible organic electronics in biology: materials and devices. *Adv. Mat.* 27 (46), 7493–7527. doi:10.1002/adma.201402625

Liu, H., Zeng, F., Tang, G., and Pan, F. (2013). Enhancement of piezoelectric response of diluted Ta doped AlN. *Appl. Surf. Sci.* 270, 225–230. doi:10.1016/j.apsusc.2013.01.005

Liu, H., Zhong, J., Lee, C., Lee, S.-W., and Lin, L. (2018). A comprehensive review on piezoelectric energy harvesting technology: materials, mechanisms, and applications. *Appl. Phys. Rev.* 5 (4). doi:10.1063/1.5074184

Liu, L., Chen, BJATSN, and Ma, H. (2020). SDCN: sensory data-centric networking for building the sensing layer of IoT. *ACM Trans. Sens. Netw.* 17 (6), 1–25. doi:10.1145/3402452

Liu, L., Ouyang, K., Chen, Z., Mo, S., Peng, Q., Jiang, L., et al. (2022c). Robust ferroelectricity enhancement of PZT thin films by a homogeneous seed layer. *J. Mater. Sci.* 57 (41), 19371–19380. doi:10.1007/s10853-022-07835-z

Liu, S., Mao, Y., Long, Y., Pan, J., Jiang, T., and Cao, M. (2022a). Applications. Key technologies of IoT intelligent sensing terminal for smart energy, 2022 IEEE International Conference on High Voltage Engineering and Applications. 25-29 Sept. 2022, Chongqing, China: ICHVE, 1–4.

Liu, X., Chen, A., Zhu, W., Li, Y., Zhang, H., Chen, Y., et al. (2023a). 20.1: invited paper: research on oxide thin film transistors for wearable sensors. *SID Symposium Dig. Tech. Pap.* 54 (S1), 151–152. doi:10.1002/sdtp.16249

Liu, Y., Dzidotor, G., Le, T. T., Vinikoor, T., Morgan, K., Curry, E. J., et al. (2022b). Exercise-induced piezoelectric stimulation for cartilage regeneration in rabbits. *Sci. Transl. Med.* 14 (627), eabi7282. doi:10.1126/scitranslmed.abi7282

Liu, Y., Yiu, C., Zhao, Z., Park, W., Shi, R., Huang, X., et al. (2023b). Soft, miniaturized, wireless olfactory interface for virtual reality. *Nat. Commun.* 14, 2297. doi:10.1038/s41467-023-37678-4

Lopez-Castaño, C., Castillo, L. F., and Corchado, J. M. (2021). Discovering the value creation system in IoT ecosystems. *sensors* 21, 328. doi:10.3390/s21020328

Luo, D., Sun, H., Li, Q., Niu, X., He, Y., and Liu, H. (2023). Flexible sweat sensors: from films to textiles. *ACS Sensors* 8 (2), 465–481. doi:10.1021/acssensors.2c02642

Luo, J. T., Fan, B., Zeng, F., and Pan, F. (2009). Influence of Cr-doping on microstructure and piezoelectric response of AlN films. *J. Phys. D Appl. Phys.* 42 (23), 235406. doi:10.1088/0022-3727/42/23/235406

Lutjes, N. R., Zhou, S., Antoja-Lleonart, J., Noheda, B., and Ocelík, V. (2021). Spherulitic and rotational crystal growth of Quartz thin films. *Sci. Rep.* 11 (1), 14888. doi:10.1038/s41598-021-94147-y

Lv, B., Zhao, G., Wang, H., Wang, Q., Yang, B., Ma, W., et al. (2023b). Ionogel fiber-based flexible sensor for friction sensing. *Adv. Mat. Technol.* 8 (10), 2201617. doi:10.1002/admt.202201617

Lv, P., Qian, J., Yang, C., Liu, T., Wang, Y., Wang, D., et al. (2022). Flexible all-inorganic Sm-doped PMN-PT film with ultrahigh piezoelectric coefficient for mechanical energy harvesting, motion sensing, and human-machine interaction. *Nano Energy* 97, 107182. doi:10.1016/j.nanoen.2022.107182

Lv, Q., Qiu, J., Zhang, H., Wen, Q., and Yu, J. (2023a). The effect and mechanism for doping concentration of Mg-Hf on the piezoelectric properties for AlN. *Mater. Res. Express* 10, 065002. doi:10.1088/2053-1591/acda13

M, W. C., Muthu, S. P., and P, R. (2020). Growth and electrical properties of self-flux method grown (1−x)Bi1/2Na1/2TiO3−xBaTiO3 single crystals across the morphotropic phase boundary. *J. Mater. Sci. Mater. Electron.* 31 (12), 9894–9903. doi:10.1007/s10854-020-03534-0

Madinei, H., Khodaparast, H. H., Adhikari, S., and Friswell, M. I. (2016). Design of MEMS piezoelectric harvesters with electrostatically adjustable resonance frequency. *Mech. Syst. Signal Process.* 81, 360–374. doi:10.1016/j.ymssp.2016.03.023

Manjakkal, L., Dervin, S., and Dahiya, R. (2020). Flexible potentiometric pH sensors for wearable systems. *RSC Adv.* 10 (15), 8594–8617. doi:10.1039/d0ra00016g

Manna, S., Talley, K. R., Gorai, P., Mangum, J., Zakutayev, A., Brennecka, G. L., et al. (2018). Enhanced piezoelectric response of AlN via CrN alloying. *Phys. Rev. Appl.* 9 (3), 034026. doi:10.1103/physrevapplied.9.034026

Mayamae, J., Vittayakorn, W., Sukkha, U., Bongkarn, T., Muanghlua, R., and Vittayakorn, N. (2017). High piezoelectric response in lead free 0.9BaTiO3-(0.1-x)CaTiO3-xBaSnO3 solid solution. *Ceram. Int.* 43, S121–S128. doi:10.1016/j.ceramint.2017.05.252

Mayrhofer, P. M., Riedl, H., Euchner, H., Stöger-Pollach, M., Mayrhofer, P. H., Bittner, A., et al. (2015). Microstructure and piezoelectric response of Y Al1−N thin films. *Acta Mater.* 100, 81–89. doi:10.1016/j.actamat.2015.08.019

Mishra, S., Mohanty, S., and Nayak, S. K. (2023). Study of nonisothermal crystallization kinetics of unstretched and uniaxially stretched electroactive PVDF composite films. *Macromol. Chem. Phys.* 224 (2), 2200326. doi:10.1002/macp.202200326

Mondal, D., Bardhan, S., Das, N., Roy, J., Ghosh, S., Maity, A., et al. (2022). Natural clay-based reusable piezo-responsive membrane for water droplet mediated energy harvesting, degradation of organic dye and pathogenic bacteria. *Nano Energy* 104, 107893. doi:10.1016/j.nanoen.2022.107893

Mondal, M. A., and Rehena, Z. J. (2022). Priority-based adaptive traffic signal control system for smart cities. *Sn Comput.Sci.* 3, 417. doi:10.1007/s42979-022-01316-5

Monereo, O., Boix, M., Claramunt, S., Prades, J. D., Cornet, A., Cirera, A., et al. (2011). Advanced performances in gas sensors: stretchable, flexible, wireless, wearable. *Procedia Eng.* 25, 1425–1428. doi:10.1016/j.proeng.2011.12.352

Mrabet, H., Belguith, S., Alhomoud, A. M., and Jemai, A. J. S. (2020). A survey of IoT security based on a layered architecture of sensing and data analysis. *Sensors* 20, 3625. doi:10.3390/s20133625

Murthy, M. N., Ganesh, V., Ravinder, G., Anusha, S., Chandrakala, G., and Sreelatha, C. J. (2023). Sol–gel synthesized ZnO thin films doped with Rb and Al for self-cleaning antibacterial applications. *J. Sol-Gel Sci. Technol.* 105 (3), 683–693. doi:10.1007/s10971-023-06044-7

Nair, K. S., Varghese, H., Chandran, A., Hareesh, U. N. S., Chouprik, A., Spiridonov, M., et al. (2022). Synthesis of KNN nanoblocks through surfactant-assisted hot injection method and fabrication of flexible piezoelectric nanogenerator based on KNN-PVDF nanocomposite. *Mater. Today Commun.* 31, 103291. doi:10.1016/j.mtcomm.2022.103291

Nakajima, T., Hanawa, S., and Tsuchiya, T. (2017). Highly stable flexible thermistor properties of spinel Mn-Co-Ni oxide films on silver/carbon micro-pinecone array composite electrodes. *J. Appl. Phys.* 122 (13). doi:10.1063/1.4994572

Nakajima, T., and Tsuchiya, T. (2015). Flexible thermistors: pulsed laser-induced liquid-phase sintering of spinel Mn–Co–Ni oxide films on polyethylene terephthalate sheets. *J. Mater. Chem. C* 3 (15), 3809–3816. doi:10.1039/c5tc00327j

Nakajima, T., and Tsuchiya, T. (2020). Ultrathin highly flexible featherweight ceramic temperature sensor arrays. *ACS Appl. Mater Interfaces* 12 (32), 36600–36608. doi:10.1021/acsami.0c08718

Namikawa, G., Shojiki, K., Yoshida, R., Kusuda, R., Uesugi, K., and Miyake, H. (2023). MOVPE growth of AlN and AlGaN films on N-polar annealed and sputtered AlN templates. *J. Cryst. Growth* 617, 127256. doi:10.1016/j.jcrysgro.2023.127256

Nasir, M., Matsumoto, H., Danno, T., Minagawa, M., Irisawa, T., Shioya, M., et al. (2006). Control of diameter, morphology, and structure of PVDF nanofiber fabricated by electrospray deposition. *J. Polym. Sci. B Polym. Phys.* 44 (5), 779–786. doi:10.1002/polb.20737

Nesser, H., Mahmoud, H. A., and Lubineau, G. (2023). High-sensitivity RFID sensor for structural health monitoring. *Adv. Sci.* 10, 2301807. doi:10.1002/advs.202301807

Ni, F., Zhu, K., Xu, L., Li, G., Liu, Y., Qian, J., et al. (2022). Manipulation of defects to achieve fast domain switching and enhance the piezoelectric properties of thin films. *Appl. Surf. Sci.* 604, 154517. doi:10.1016/j.apsusc.2022.154517

Niu, X., Zhou, S., Pan, D., Zhao, Y., and Li, L. (2022). Insight into the role of debris in the formation of polytetrafluoroethylene film via molecular dynamic simulation of debris adhesion. *Polym. Eng. Sci.* 62 (11), 3672–3683. doi:10.1002/pen.26136

Okayasu, M., and Watanabe, K. (2016). A study of the electric power generation properties of a lead zirconate titanate piezoelectric ceramic. *Ceram. Int.* 42 (12), 14049–14060. doi:10.1016/j.ceramint.2016.06.012

Pandey, R. K., Hossain, M. D., Moriyama, S., and Higuchi, M. (2014). Real-time humidity-sensing properties of ionically conductive Ni(ii)-based metallo-supramolecular polymers. *J. Mater. Chem. A* 2 (21), 7754–7758. doi:10.1039/c4ta00884g

Park, I.-J., Jeong, C.-Y., Cho, I.-T., Lee, J.-H., Cho, E.-S., Kwon, S. J., et al. (2012). Fabrication of amorphous InGaZnO thin-film transistor-driven flexible thermal and pressure sensors. *Semicond. Sci. Technol.* 27 (10), 105019. doi:10.1088/0268-1242/27/10/105019

Park, M., Park, Y. J., Chen, X., Park, Y.-K., Kim, M.-S., and Ahn, J.-H. (2016). MoS2-Based tactile sensor for electronic skin applications. *Adv. Mat.* 28 (13), 2556–2562. doi:10.1002/adma.201505124

Patidar, J., Sharma, A., Zhuk, S., Lorenzin, G., Cancellieri, C., Sarott, M. F., et al. (2023). Improving the crystallinity and texture of oblique-angle-deposited AlN thin films using reactive synchronized HiPIMS. *Surf. Coatings Technol.* 468, 129719. doi:10.1016/j.surfcoat.2023.129719

Petritz, A., Karner-Petritz, E., Uemura, T., Schäffner, P., Araki, T., Stadlober, B., et al. (2021). Imperceptible energy harvesting device and biomedical sensor based on ultraflexible ferroelectric transducers and organic diodes. *Nat. Commun.* 12 (1), 2399. doi:10.1038/s41467-021-22663-6

Portilla, L., Loganathan, K., Faber, H., Eid, A., Hester, J. G. D., Tentzeris, M. M., et al. (2023). Wirelessly powered large-area electronics for the Internet of Things. *Nat. Electron.* 6 (1), 10–17. doi:10.1038/s41928-022-00898-5

Qiao, H., Zhang, Y., Huang, Z., Wang, Y., Li, D., and Zhou, H. (2018). 3D printing individualized triboelectric nanogenerator with macro-pattern. *Nano Energy* 50, 126–132. doi:10.1016/j.nanoen.2018.04.071

Rim, Y. S., Bae, S.-H., Chen, H., Yang, J. L., Kim, J., Andrews, A. M., et al. (2015). Printable ultrathin metal oxide semiconductor-based conformal biosensors. *ACS Nano* 9 (12), 12174–12181. doi:10.1021/acsnano.5b05325

Russell, T., Shafiee, A., Conley, B., and Sadeghi, F. (2022). Evaluating load distribution at the bearing-housing interface using thin film pressure sensors. *Tribol. Int.* 165, 107293. doi:10.1016/j.triboint.2021.107293

Sabry, R. S., and Hussein, A. D. (2019). PVDF: ZnO/BaTiO3 as high out-put piezoelectric nanogenerator. *Polym. Test.* 79, 106001. doi:10.1016/j.polymertesting.2019.106001

Safari, A., Zhou, Q., Zeng, Y., and Leber, J. D. (2023). Advances in development of Pb-free piezoelectric materials for transducer applications. *Jpn. J. Appl. Phys.* 62 (SJ), SJ0801. doi:10.35848/1347-4065/acc812

Saikh, M. M., Hoque, N. A., Biswas, P., Rahman, W., Das, N., Das, S., et al. (2021). Self-polarized ZrO2/Poly(vinylidene fluoride-co-hexafluoropropylene) nanocomposite-based piezoelectric nanogenerator and single-electrode triboelectric nanogenerator for sustainable energy harvesting from human movements. *Phys. status solidi (a)* 218, 2000695. doi:10.1002/pssa.202000695

Santos, L., Neto, J. P., Crespo, A., Nunes, D., Costa, N., Fonseca, I. M., et al. (2014). WO3 nanoparticle-based conformable pH sensor. *ACS Appl. Mater. Interfaces* 6 (15), 12226–12234. doi:10.1021/am501724h

Sapkota, B., Hasan, M. T., Martin, A., Mahbub, R., Shield, J. E., and Rangari, V. (2022). Fabrication and magnetoelectric investigation of flexible PVDF-TrFE/cobalt ferrite nanocomposite films. *Mater. Res. Express* 9 (4), 046302. doi:10.1088/2053-1591/ac6151

Sarkar, D., Das, N., Saikh, M. M., Biswas, P., Das, S., Das, S., et al. (2021). Development of a sustainable and biodegradable *Sonchus asper* cotton pappus based piezoelectric nanogenerator for instrument vibration and human body motion sensing with mechanical energy harvesting applications. *ACS Omega* 6, 28710–28717. doi:10.1021/acsomega.1c03374

Sarkar, D., Das, N., Saikh, M. M., Biswas, P., Roy, S., Paul, S., et al. (2023b). High β-crystallinity comprising nitrogenous carbon dot/PVDF nanocomposite decorated self-powered and flexible piezoelectric nanogenerator for harvesting human movement mediated energy and sensing weights. *Ceram. Int.* 49, 5466–5478. doi:10.1016/j.ceramint.2022.10.070

Sarkar, D., Das, N., Saikh, M. M., Roy, S., Paul, S., Hoque, N. A., et al. (2023a). Elevating the performance of nanoporous bismuth selenide incorporated arch-shaped triboelectric nanogenerator by implementing piezo-tribo coupling effect: harvesting biomechanical energy and low scale energy sensing applications. *Adv. Compos. Hybrid Mater.* 6, 232. doi:10.1007/s42114-023-00807-0

Sarkar, D., Das, N., Sau, S., Basu, R., and Das, S. (2024). Micro-patterned BaTiO3@Ecoflex nanocomposite-assisted self-powered and wearable triboelectric nanogenerator with improved charge retention by 2D MoTe2/PVDF nanofibrous layer. *J. Mater. Chem. C* 12, 984–1001. doi:10.1039/D3TC03822J

Satake, Y., Fujiwara, K., Shiogai, J., Seki, T., and Tsukazaki, A. (2019). Fe-Sn nanocrystalline films for flexible magnetic sensors with high thermal stability. *Sci. Rep.* 9 (1), 3282. doi:10.1038/s41598-019-39817-8

Satapathy, S., Pawar, S., Gupta, P. K., and Varma, K. B. R. (2011). Effect of annealing on phase transition in poly(vinylidene fluoride) films prepared using polar solvent. *Bull. Mater. Sci.* 34 (4), 727–733. doi:10.1007/s12034-011-0187-0

Shalabi, N., Searles, K., and Takahata, K. (2022). Switch mode capacitive pressure sensors. *Microsystems Nanoeng.* 8 (1), 132. doi:10.1038/s41378-022-00469-w

Sharma, S., Kumar, A., Gupta, V., and Tomar, M. (2019). Dielectric and ferroelectric studies of KNN thin film grown by pulsed laser deposition technique. *Vacuum* 160, 233–237. doi:10.1016/j.vacuum.2018.11.036

Shi, E., Yuan, B., Shiring, S. B., Gao, Y., Akriti, G. Y., Su, C., et al. (2020). Two-dimensional halide perovskite lateral epitaxial heterostructures. *Nature* 580 (7805), 614–620. doi:10.1038/s41586-020-2219-7

Shi, J., Liu, J., Xie, S., Chen, K., Zheng, H., Wu, B., et al. (2023). Dopant tuned multi-functionality in barium titanate based lead-free piezoceramics. *J. Alloys Compd.* 942, 169092. doi:10.1016/j.jallcom.2023.169092

Shi, K., Sun, B., Huang, X., and Jiang, P. (2018). Synergistic effect of graphene nanosheet and BaTiO3 nanoparticles on performance enhancement of electrospun PVDF nanofiber mat for flexible piezoelectric nanogenerators. *Nano Energy* 52, 153–162. doi:10.1016/j.nanoen.2018.07.053

Shin, J., Jeong, B., Kim, J., Nam, V. B., Yoon, Y., Jung, J., et al. (2020). Sensitive wearable temperature sensor with seamless monolithic integration. *Adv. Mat.* 32 (2), 1905527. doi:10.1002/adma.201905527

Shirvanimoghaddam, M., Johnson, S. J., and Lance, A. M. (2016). "Design of Raptor codes in the low SNR regime with applications in quantum key distribution," in 2016 IEEE International Conference on Communications (ICC), USA, 22-27 May 2016 (IEEE), 1–6.

Siang, J., Lim, M. H., and Salman, L. M. (2018). Review of vibration-based energy harvesting technology: mechanism and architectural approach. *Int. J. Energy Res.* 42 (5), 1866–1893. doi:10.1002/er.3986

Silvano, W. F., and Marcelino, R. J. (2020). Iota Tangle: a cryptocurrency to communicate Internet-of-Things data. *Future Gener. Comput. Syst.* 112, 307–319. doi:10.1016/j.future.2020.05.047

Singh, D., Choudhary, A., and Garg, A. (2018). Flexible and robust piezoelectric polymer nanocomposites based energy harvesters. *ACS Appl. Mater. Interfaces* 10, 2793–2800. doi:10.1021/acsami.7b16973

Song, J.-Y., Yu, P.-L., and Li, J.-C. (2022). Low-temperature bending fatigue of MXene/PDMS flexible pressure sensor. *Adv. Mat.* 9 (32), 2201463. doi:10.1002/admi.202201463

Sonklin, T., Munthala, D., Leuasoongnoen, P., Janphuang, P., and Pojprapai, S. (2022). Effect of substrate-tilting angle-dependent grain growth and columnar growth in ZnO film deposited using radio frequency (RF) magnetron sputtering method. *J. Mater. Sci. Mater. Electron.* 33 (21), 16977–16986. doi:10.1007/s10854-022-08576-0

A strategy for obtaining AlN (2023). A strategy for obtaining AlN heteroepitaxial films with high crystalline quality. *Nat. Mater.* 22, 816–817. doi:10.1038/s41563-023-01574-5

Sugahara, T., Alipour, L., Hirose, Y., Ekubaru, Y., Nakamura, J.-i., Ono, H., et al. (2020). Formation of metal-organic decomposition derived nanocrystalline structure titanium dioxide by heat sintering and photosintering methods for advanced coating process, and its volatile organic compounds' gas-sensing properties. *ACS Appl. Electron. Mater.* 2 (6), 1670–1678. doi:10.1021/acsaelm.0c00237

Sun, Y., Chen, J., Li, X., Lu, Y., Zhang, S., and Cheng, Z. (2019). Flexible piezoelectric energy harvester/sensor with high voltage output over wide temperature range. *Nano Energy* 61, 337–345. doi:10.1016/j.nanoen.2019.04.055

Sun, Y., Gao, X., A, S., Fang, H., Lu, M., Yao, D., et al. (2023). Hydrophobic multifunctional flexible sensors with a rapid humidity response for long-term respiratory monitoring. *ACS Sustain. Chem. Eng.* 11 (6), 2375–2386. doi:10.1021/acssuschemeng.2c06162

Swagata, R., Pradip, T., Hoque, N. A., Biswajoy, B., Nayim, S., Farha, K., et al. (2017). Electroactive and high dielectric folic acid/PVDF composite film rooted simplistic organic photovoltaic self-charging energy storage cell with superior energy density and storage capability. *ACS Appl. Mat. Interfaces* 9, 24198–24209. doi:10.1021/acsami.7b05540

Tai, D., Zhao, X., Zheng, T., and Wu, J. (2023). Establishing a relationship between the piezoelectric response and oxygen vacancies in lead-free piezoelectrics. *ACS Appl. Mater. Interfaces* 15 (30), 36564–36575. doi:10.1021/acsami.3c06520

Takahashi, Y., and Tadokoro, H. (1980). Crystal structure of form III of poly(vinylidene fluoride). *Macromolecules* 13 (5), 1317–1318. doi:10.1021/ma60077a057

Tan, G., Maruyama, K., Kanamitsu, Y., Nishioka, S., Ozaki, T., Umegaki, T., et al. (2019). Crystallographic contributions to piezoelectric properties in PZT thin films. *Sci. Rep.* 9 (1), 7309. doi:10.1038/s41598-019-43869-1

Tekcin, M., Paker, S., and Bahadir, S. K. (2022). UHF-RFID enabled wearable flexible printed sensor with antenna performance. *AEU - Int. J. Electron. Commun.* 157, 154410. doi:10.1016/j.aeue.2022.154410

Terai, Y., Haraguchi, K., Ichinose, R., Oota, H., and Yonezawa, K. (2023). Structural and piezoelectric properties of AlN thin films grown by pressure gradient sputtering. *Jpn. J. Appl. Phys.* 62 (SA), SA1003. doi:10.35848/1347-4065/ac762f

Teymourian, H., Barfidokht, A., and Wang, J. (2020). Electrochemical glucose sensors in diabetes management: an updated review (2010–2020). *Chem. Soc. Rev.* 49 (21), 7671–7709. doi:10.1039/d0cs00304b

Toma, M., Domokos, R., Lung, C., Marconi, D., and Pop, M. (2023). Characterization of ZnO, Ga-doped ZnO, and Nd-Ga-doped ZnO thin films synthesized by radiofrequency magnetron sputtering. *Anal. Lett.* 57, 797–811. doi:10.1080/00032719.2023.2225199

Tripathy, A., Maria Joseph Raj, N. P., Saravanakumar, B., Kim, S.-J., and Ramadoss, A. (2023). Tuning of highly piezoelectric bismuth ferrite/PVDF-copolymer flexible films for efficient energy harvesting performance. *J. Alloys Compd.* 932, 167569. doi:10.1016/j.jallcom.2022.167569

Trudeau, C., Beaupré, P., Bolduc, M., and Cloutier, S. G. (2020). All inkjet-printed perovskite-based bolometers. *npj Flex. Electron.* 4 (1), 34. doi:10.1038/s41528-020-00097-2

Tsakanikas, V., Dagiuklas, T., Iqbal, M., Wang, X., and Mumtaz, S. (2023). An intelligent model for supporting edge migration for virtual function chains in next generation internet of things. *Sci. Rep.* 13 (1), 1063. doi:10.1038/s41598-023-27674-5

Uslu, B. Ç., Okay, E., and EjjoCC, D. (2020). Analysis of factors affecting IoT-based smart hospital design. *J. Cloud Comp.* 9, 67. doi:10.1186/s13677-020-00215-5

Wang, C., and Li, Z. (2016). A review of start-up circuits for low voltage self-powered DC-type energy harvesters. *J.Circuits Syst.Comput.* 25 (07), 1630003. doi:10.1142/s0218126616300038

Wang, D. W., Mo, J. L., Wang, X. F., Ouyang, H., and Zhou, Z. R. (2018). Experimental and numerical investigations of the piezoelectric energy harvesting via friction-induced vibration. *Energy Convers. Manag.* 171, 1134–1149. doi:10.1016/j.enconman.2018.06.052

Wang, S., Chen, C., Wang, J., Li, C.-B.-W., Zhou, J., Liu, Y.-X., et al. (2022). Synergetic chemo-piezodynamic therapy of osteosarcoma enabled by defect-driven lead-free piezoelectrics. *Adv. Funct. Mat.* 32 (44), 2208128. doi:10.1002/adfm.202208128

Wang, S., Wang, Y., Wang, Z., Wu, Z., Xin, Y., and Zhou, X. (2023a). A brief review on hydrophone based on PVDF piezoelectric film. *Ferroelectrics* 603 (1), 150–156. doi:10.1080/00150193.2022.2159227

Wang, W., Asci, C., Zeng, W., and Sonkusale, S. (2023c). Zero-power screen printed flexible RFID sensors for Smart Home. *J. Ambient Intell. Humaniz. Comput.* 14 (4), 3995–4004. doi:10.1007/s12652-022-04466-9

Wang, X. (2012). Piezoelectric nanogenerators—harvesting ambient mechanical energy at the nanometer scale. *Nano Energy* 1 (1), 13–24. doi:10.1016/j.nanoen.2011.09.001

Wang, X., Liu, X., Ge, X., and Schubert, D. W. (2023b). Superior sensitive, high-tensile flexible fabric film strain sensor. *Compos. Part A Appl. Sci. Manuf.* 172, 107610. doi:10.1016/j.compositesa.2023.107610

Wang, Y., Xu, Y., Dong, S., Wang, P., Chen, W., Lu, Z., et al. (2021). Ultrasonic activation of inert poly(tetrafluoroethylene) enables piezocatalytic generation of reactive oxygen species. *Nat. Commun.* 12 (1), 3508. doi:10.1038/s41467-021-23921-3

Wen, D., Shen, Y., Sun, P., Huang, J., Gu, F., and Wang, L. (2022). Defect regulation of AlN films based on Al-rich AlN targets. *Semicond. Sci. Technol.* 37 (10), 105001. doi:10.1088/1361-6641/ac889a

Won, S. S., Kawahara, M., Glinšek, S., Lee, J., Kim, Y., Jeong, C. K., et al. (2018). Flexible vibrational energy harvesting devices using strain-engineered perovskite piezoelectric thin films. *Nano Energy* 55, 182–192. doi:10.1016/j.nanoen.2018.10.068

Wu, B., Wu, H., Wu, J., Xiao, D., Zhu, J., and Pennycook, S. J. (2016). Giant piezoelectricity and high Curie temperature in nanostructured alkali niobate lead-free piezoceramics through phase coexistence. *J. Am. Chem. Soc.* 138 (47), 15459–15464. doi:10.1021/jacs.6b09024

Wu, F., Li, Y., Zhang, H., Jiang, H., Wei, W., and Deng, C. (2023). Self-powered ultra-flexible infrared sensor based on PVA-PEDOT: PSS/Ti3C2Tx composite film. *Appl. Surf. Sci.* 639, 158212. doi:10.1016/j.apsusc.2023.158212

Wu, N., Wang, Q., and Xie, X. (2015). Ocean wave energy harvesting with a piezoelectric coupled buoy structure. *Appl. Ocean Res.* 50, 110–118. doi:10.1016/j.apor.2015.01.004

Xie, X., Zhou, Z., Gao, B., Zhou, Z., Liang, R., and Dong, X. (2022). Ion-pair engineering-induced high piezoelectricity in Bi4Ti3O12-based high-temperature piezoceramics. *ACS Appl. Mater. Interfaces* 14 (12), 14321–14330. doi:10.1021/acsami.1c19445

Xie, X. D., and Wang, Q. (2015). Energy harvesting from a vehicle suspension system. *Energy* 86, 385–392. doi:10.1016/j.energy.2015.04.009

Xu, G., Luo, H., Wang, P., Xu, H., and Yin, Z. (2000). Ferroelectric and piezoelectric properties of novel relaxor ferroelectric single crystals PMNT. *Chin. Sci. Bull.* 45 (6), 491–495. doi:10.1007/bf02887091

Yamamoto, Y., Harada, S., Yamamoto, D., Honda, W., Arie, T., Akita, S., et al. (2016). Printed multifunctional flexible device with an integrated motion sensor for health care monitoring. *Sci. Adv.* 2 (11), e1601473. doi:10.1126/sciadv.1601473

Yan, J., Liu, M., Jeong, Y. G., Kang, W., Li, L., Zhao, Y., et al. (2019). Performance enhancements in poly(vinylidene fluoride)-based piezoelectric nanogenerators for efficient energy harvesting. *Nano Energy* 56, 662–692. doi:10.1016/j.nanoen.2018.12.010

Yan, W., Ma, C., Cai, X., Sun, Y., Zhang, G., and Song, W. (2023). Self-powered and wireless physiological monitoring system with integrated power supply and sensors. *Nano Energy* 108, 108203. doi:10.1016/j.nanoen.2023.108203

Yanagitani, T., and Jia, J. (2019). "ScAlN polarization inverted resonators and enhancement of kt2 in new YbAlN materials for BAW devices," in 2019 IEEE International Ultrasonics Symposium (IUS), USA, 6-9 Oct. 2019 (IEEE), 894–899.

Yang, F., Li, J., Long, Y., Zhang, Z., Wang, L., Sui, J., et al. (2021). Wafer-scale heterostructured piezoelectric bio-organic thin films. *Science* 373 (6552), 337–342. doi:10.1126/science.abf2155

Yang, F., Yuan, Z., Wu, S., Chen, J., Hou, M., Liu, A., et al. (2023). Energy storage performance of PZT/PZ composite films obtained by sol–gel method. *Phys. Status Solidi A* 220 (17), 2300233. doi:10.1002/pssa.202300233

Yang, L., Cheng, M., Lyu, W., Shen, M., Qiu, J., Ji, H., et al. (2018). Tunable piezoelectric performance of flexible PVDF based nanocomposites from MWCNTs/graphene/MnO2 three-dimensional architectures under low poling electric fields. *Compos. Part A Appl. Sci. Manuf.* 107, 536–544. doi:10.1016/j.compositesa.2018.02.004

Ye, L., Chen, L., Yu, J., Tu, S., Yan, B., Zhao, Y., et al. (2021). High-performance piezoelectric nanogenerator based on electrospun ZnO nanorods/P(VDF-TrFE) composite membranes for energy harvesting application. *J. Mater. Sci. Mater. Electron.* 32 (4), 3966–3978. doi:10.1007/s10854-020-05138-0

Yen, C.-K., Dutt, K., Yao, Y.-S., Wu, W.-J., Shiue, Y.-L., Pan, C.-T., et al. (2022). Development of flexible biceps tremors sensing chip of PVDF fibers with nano-silver particles by near-field electrospinning. *Polymers* 14 (2), 331. doi:10.3390/polym14020331

Yu, J., Xian, S., Mu, J., Wang, M., Wang, Y., Hou, X., et al. (2023). Hybrid electromechanical properties of hetero-doped and homogeneously bonded dual-mode pressure sensor for indoor body area network node. *Sci. China Inf. Sci.* 67 (1), 112401. doi:10.1007/s11432-023-3801-1

Yuan, C., Zhang, C., Yang, C., Wu, F., Xiao, S., and Sun, H. (2023). Enhanced piezoelectric properties of poly(vinylidene fluoride)/lead zirconate titanate (PVDF/PZT) fiber films fabricated by electrospinning. *J. Electron. Mater.* 52, 7193–7207. doi:10.1007/s11664-023-10631-3

Yue, Y., Liu, N., Su, T., Cheng, Y., Liu, W., Lei, D., et al. (2023). Self-powered nanofluidic pressure sensor with a linear transfer mechanism. *Adv. Funct. Mat.* 33 (13), 2211613. doi:10.1002/adfm.202211613

Zakria, H. S., Othman, M. H. D., Kamaludin, R., Jilani, A., Omar, M. F., Ayub, M., et al. (2023). Removal of bisphenol A from synthetic and treated sewage wastewater using magnetron sputtered CuxO/PVDF thin film photocatalytic hollow fiber membrane. *J. Water Process Eng.* 51, 103425. doi:10.1016/j.jwpe.2022.103425

Zang, Y., Huang, D., Di, C.-a., and Zhu, D. (2016). Device engineered organic transistors for flexible sensing applications. *Adv. Mat.* 28 (22), 4549–4555. doi:10.1002/adma.201505034

Zha, X.-H., Ma, X., Luo, J.-T., and Fu, C. (2023). Enhanced piezoelectric response of AlN via alloying of transitional metals, and influence of type and distribution of transition metals. *Nano Energy* 111, 108390. doi:10.1016/j.nanoen.2023.108390

Zhang, C., Yuan, C., Zhu, Q., and Sun, H. (2023c). Large-scale fabrication and performance improvement of polyvinylidene fluoride piezoelectric composite films. *Ceram. Int.* 49 (16), 27255–27265. doi:10.1016/j.ceramint.2023.05.280

Zhang, M.-H., Shen, C., Zhao, C., Dai, M., Yao, F.-Z., Wu, B., et al. (2022a). Deciphering the phase transition-induced ultrahigh piezoresponse in (K,Na)NbO3-based piezoceramics. *Nat. Commun.* 13 (1), 3434. doi:10.1038/s41467-022-31158-x

Zhang, Q., Sánchez-Fuentes, D., Gómez, A., Desgarceaux, R., Charlot, B., Gàzquez, J., et al. (2019). Tailoring the crystal growth of quartz on silicon for patterning epitaxial piezoelectric films. *Nanoscale Adv.* 1 (9), 3741–3752. doi:10.1039/c9na00388f

Zhang, Q., Xu, M., Zhou, L., Shihao, L., Wang, W., Zhang, L., et al. (2023b). A flexible organic mechanoluminophore device. *Nat. Commun.* 14, 1257. doi:10.1038/s41467-023-36916-z

Zhang, S., Zheng, Y., Lu, Y., Xie, B., Chen, D., Wang, J., et al. (2021a). A micromachined resonant micro-pressure sensor. *IEEE Sensors J.* 21 (18), 19789–19796. doi:10.1109/jsen.2021.3091843

Zhang, Y., Chen, X., and Shen, Z. (2023a). Internet use, market transformation, and individual tolerance: evidence from China. *Humanit. Soc. Sci. Commun.* 10, 273. doi:10.1057/s41599-023-01781-0

Zhang, Z., Li, X., Peng, Z., Yan, X., Liu, S., Hong, Y., et al. (2023d). Active self-assembly of piezoelectric biomolecular films via synergistic nanoconfinement and *in-situ* poling. *Nat. Commun.* 14 (1), 4094. doi:10.1038/s41467-023-39692-y

Zhang, Z., Liu, S., Pan, Q., Hong, Y., Shan, Y., Peng, Z., et al. (2022b). Van der Waals Exfoliation Processed Biopiezoelectric Submucosa Ultrathin Films. *Adv. Mat.* 34 (26), 2200864. doi:10.1002/adma.202200864

Zhang, Z., Lu, S., Cai, R., and Tan, W. (2021b). Rapid water-responsive shape memory films for smart resistive bending sensors. *Nano Today* 38, 101202. doi:10.1016/j.nantod.2021.101202

Zhao, J., Han, J., Xing, Y., Lin, W., Yu, L., Cao, X., et al. (2020b). Fabrication and application of flexible AlN piezoelectric film. *Semicond. Sci. Technol.* 35 (3), 035009. doi:10.1088/1361-6641/ab6bb0

Zhao, X., Zhang, W., Chen, S., Zhang, J., and Wang, X. (2012). Hydrophilicity and crystallization behavior of PVDF/PMMA/TiO2(SiO2) composites prepared by *in situ* polymerization. *J. Polym. Res.* 19 (5), 9862. doi:10.1007/s10965-012-9862-0

Zhao, Y., Wang, B., Hojaiji, H., Wang, Z., Lin, S., Yeung, C., et al. (2020a). A wearable freestanding electrochemical sensing system. *Sci. Adv.* 6 (12), eaaz0007. doi:10.1126/sciadv.aaz0007

Zhou, W., He, Q., Ye, H., Ye, C., Wu, X., and Chu, J. (2021). Recent advances in flexible sweat glucose biosensors. *J. Phys. D Appl. Phys.* 54 (42), 423001. doi:10.1088/1361-6463/ac14ef

Zhou, X., Parida, K., Halevi, O., Liu, Y., Xiong, J., Magdassi, S., et al. (2020). All 3D-printed stretchable piezoelectric nanogenerator with non-protruding kirigami structure. *Nano Energy* 72, 104676. doi:10.1016/j.nanoen.2020.104676

Zu, H., Wu, H., and Wang, Q. M. (2016). High-temperature piezoelectric crystals for acoustic wave sensor applications. *IEEE Trans. Ultrasonics, Ferroelectr. Freq. Control* 63 (3), 486–505. doi:10.1109/tuffc.2016.2527599